CAL-2038

National Aeronautics and Space Administration

ANNUAL STATUS REPORT
FOR NASA GRANT NAGW-2013

Submitted to:

Astrophysics Division
Code SZC
National Aeronautics and Space Administration
Washington, DC 20546

Submitted by:

The Trustees of Columbia University
in the City of New York
Box 20, Low Memorial Library
New York, New York 10027

Prepared by:

Columbia Astrophysics Laboratory
Departments of Astronomy and Physics
Columbia University
538 West 120th Street
New York, New York 10027

Title of Research:

"Development of a High Resolution Liquid Xenon Imaging Telescope for Medium Energy Gamma-Ray Astrophysics"

Principal Investigator:

Professor Elena Aprile
Columbia University

Period covered by Report:

1 January 1992 – 31 December 1992

December 1992

NASA Report 92

In the third year of the research project entitled "Development of a High Resolution Liquid Xenon Imaging Telescope for Medium Energy Gamma-Ray Astrophysics" (NAGW-2013), we have tested a 3.5 liter prototype of the Liquid Xenon Time Projection Chamber. After having successfully purified the 3.5 liter of liquid xenon, we have used a prototype having a 4.4 cm drift gap to study the charge and energy resolution response of the 3.5 liter chamber. We have obtained an energy resolution as good as that previously measured by us using chambers with drift gaps of the order of millimeters. We have observed the induction signals produced by MeV gamma-rays, using a sense wire configuration similar to that originally proposed by Gatti et al. in 1970. We have used the 20 hybrid charge sensitive preamplifiers, that were tested in the second year of this research project, for a non-destructive readout of the electron image on the induction wires. We have also performed extensive Monte Carlo simulations to obtain results on efficiency, background rejection capability, and source flux sensitivity, and have developed a reconstruction algorithm for events with multiple interaction points. For these studies we have assumed a coded aperture mask at a distance of 1 m from the Liquid Xenon Time Projection Chamber.

These results have been presented at the "International Conference on Liquid Radiation Detectors", held in Tokyo on April 7-10, 1992, at the "3rd International Conference on Advanced Technology and Particle Physics", held in Como, Italy on June 22-26, 1992, and at the "Gamma-Ray Detectors" conference of the SPIE's International Symposium on Optical Engineering, held in San Diego on July 19-24, 1992.

For a more complete description of the results obtained in the third year of the project, three preprints submitted for publication in *Nuclear Instruments and Methods*, *Nuclear Physics B (Proc. Suppl.)* and *SPIE Conference Proceedings* are attached as Appendices A, B, and C, respectively.

APPENDIX A

A MONTE CARLO ANALYSIS OF THE LIQUID XENON TPC AS GAMMA-RAY TELESCOPE

E. Aprile, A. Bolotnikov, D. Chen and R. Mukherjee
Department of Physics and
Columbia Astrophysics Laboratory, Columbia University
538 West 120th Street, New York, NY 10027, USA

Presented at the:
"International Conference on Liquid Radiation Detectors"
April 7 - 10, 1992, Waseda University, Tokyo, Japan

To appear in:
Nuclear Instruments and Methods in Physics Research A, 1992

COLUMBIA UNIVERSITY

DEPARTMENTS OF

PHYSICS and ASTRONOMY

NEW YORK, NEW YORK 10027

Columbia Astrophysics Laboratory Contribution Number 493

A MONTE CARLO ANALYSIS OF THE LIQUID XENON TPC AS GAMMA-RAY TELESCOPE

E. Aprile, A. Bolotnikov, D. Chen and R. Mukherjee
Physics Department and
Columbia Astrophysics Laboratory
Columbia University, New York, NY 10027

ABSTRACT

Extensive Monte Carlo modeling of a coded aperture γ-ray telescope based on a high resolution liquid xenon TPC has been performed. Results on efficiency, background reduction capability and source flux sensitivity are presented. We discuss in particular the development of a reconstruction algorithm for events with multiple interaction points. From the energy and spatial information, the kinematics of Compton scattering is used to identify and reduce background events, as well as to improve the detector response in the few MeV region. Assuming a spatial resolution of 1 mm RMS and an energy resolution of 4.5% FWHM at 1 MeV, the algorithm is capable of reducing by an order of magnitude the background rate expected at balloon altitude, thus significantly improving the telescope sensitivity.

1. INTRODUCTION

Significant progress in experimental γ-ray astrophysics can only be achieved with the development of instruments with improved imaging capability. Efforts to improve the sensitivity of a γ-ray telescope without a corresponding improvement in angular resolution will result in source confusion in the field-of-view (FOV) and will limit the mapping of extended source distributions. Two important scientific objectives which typify the need for detectors with improved imaging capability, along with good sensitivity and energy resolution, are the 1.8 MeV line emission from radioactive ^{26}Al and the 0.511 MeV positron-electron annihilation emission. For both cases a precise study of the spatial distribution of the emission will uniquely identify the sources of radiation. Among the proposed novel techniques for imaging astrophysical γ-ray sources in the low to medium energy region, the liquid xenon Time Projection Chamber (LXe-TPC) is recognized as very promising and worth a strong R&D effort. Like an electronic bubble chamber, a TPC is capable of visualizing the complex histories of γ-ray events with multiple interactions, initiated by either Compton scattering or pair production. As a result of this imaging, efficient background rejection is also achieved, reducing the requirement for a massive anti-coincidence shield of the type that is required for germanium and sodium iodide detectors. From the energy and spatial information available for each point of interaction, Compton kinematics enables the reconstruction of the direction of the incoming γ-ray. The direction is not unique unless the Compton scattered electron is also imaged. Given the short range of low energy electrons in liquid xenon, this is not possible for a practical spatial resolution of the order of millimeters. In the LXe-TPC Compton telescope, as proposed by us in [1], the angular resolution for the MeV region is limited by the small separation between two successive γ-ray interactions.

To overcome this limitation and release the strong requirement on the TPC spatial resolution, we propose to combine the imaging capability of the LXe-TPC with that of the coded aperture technique, for studying astrophysical sources in the few MeV region with arcminute accuracy. In a coded aperture telescope, a mask consisting of a two-dimensional array of opaque and transparent elements is placed between the source and a position sensitive γ-ray detector. Every source within the FOV casts a shadow of part of the mask onto the detector. By properly decoding the pattern obtained at the detector plane, an image of the source is inferred. The successful application of coded aperture imaging in the low energy γ-ray region has been demonstrated by two balloon borne telescopes : the New Hampshire "Directional Gamma-Ray Telescope", DGT [2] and the Caltech "Gamma-Ray Imaging Payload", GRIP [3], and more recently by the SIGMA telescope aboard the GRANAT satellite [4]. All these telescopes use scintillators as position sensitive γ-ray detectors. The advantage of the LXe-TPC/coded telescope is in its unique capability to suppress background over a wide energy range, thus improving the sensitivity to weak sources, while maintaining an excellent detection efficiency, energy and angular resolution.

In this paper the technical aspects of the LXe-TPC development are not considered. For this we refer to previous publications by Aprile et al. [5]. We present here initial results from a Monte Carlo analysis of the expected performance of the LXe-TPC coupled to a coded aperture as γ-ray telescope for 0.3-10 MeV.

2. MONTE CARLO ANALYSIS AND RESULTS

2.1 Telescope Model

The model of the γ-ray telescope used in the Monte Carlo simulation is schematically shown in Fig.1. It consists of a coded aperture mask, located 1 meter above the LXe-TPC γ-ray detector. An active CsI shield has been included. In practice, the background rejection capability

of the TPC reduces the need for massive anti-coincidence shield. The sensitive area of the TPC is 39 x 28 cm^2. The total depth of liquid xenon is 10 cm. The detector's dimensions and mask-detector separation have been determined on the basis of the existing gondola for the DGT telescope that we plan to use for the first balloon flight of the telescope [6]. The TPC is operated in the ionization mode. Both the energy and the spatial distribution of each ionizing event within its sensitive volume is measured. The coordinates in the X-Y plane are inferred from the signals induced on two orthogonal wire planes, while the coordinate along the Z-direction is inferred from the drift time measured with respect to a zero time provided by the fast scintillation signal. As indicated by our first experimental results on the induction signals in a 3.5 liter LXe-TPC, to be published elsewhere, the spatial resolution in the plane is better than $S/\sqrt{12}$ where S is the spacing between the induction wires. For the spatial resolution on the coordinate along the drift axis we have previously measured $\sigma_z = 0.18$ mm [5]. For the Monte Carlo calculations, a resolution of $\sigma_x = \sigma_y = 1$ mm and $\sigma_z = 0.2$ mm has been assumed, along with the experimental energy resolution of 4.5% FWHM at 1 MeV, extrapolated according to a $E^{-1/2}$ law [7].

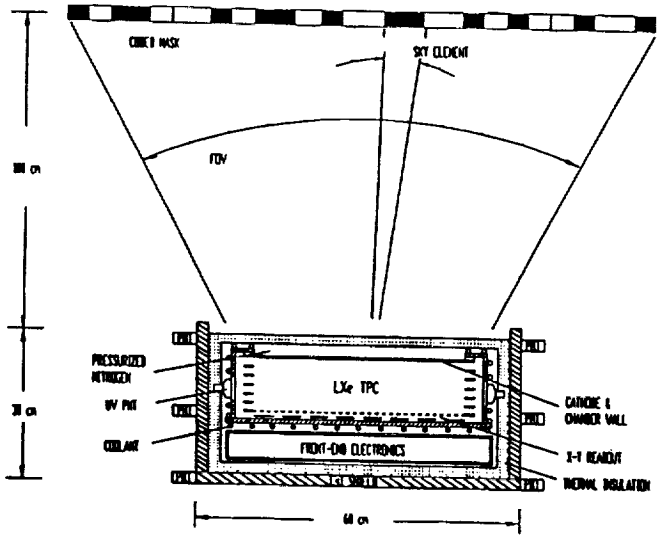

Fig. 1. Schematic of the LXe-TPC/coded mask γ-ray telescope.

The mask is a 2 x 2 mosaic of a basic Uniformly Redundant Array (URA) [8]. It consists of a 43 x 41 element pattern of 0.91 cm x 0.68 cm x 1.2 cm thick tungsten blocks. With the assumed separation of 1 meter between mask and the detector, an angular pixel size of 0.65° x 0.49° and a FOV of 28° x 20° is defined. Much finer angular resolution is obtained by increasing the mask-detector separation. The precision in point source localization depends, however, also on the detector's spatial resolution and the statistical significance of the source data. We have estimated that a precision at the arcminute level is possible with a practical spatial resolution of 1 or 2 mm.

2.2 Reconstruction Algorithm based on Compton Kinematics

The interaction of γ-rays in liquid xenon is dominated by Compton scattering and pair production, for energies larger than few hundred keV. The typical event registered by the TPC is therefore characterized by multiple interaction points before the original γ-ray energy is fully deposited in the liquid. This is illustrated in Fig. 2 where the distribution of the number of interaction points for three different γ-ray energies is plotted. The probability that the

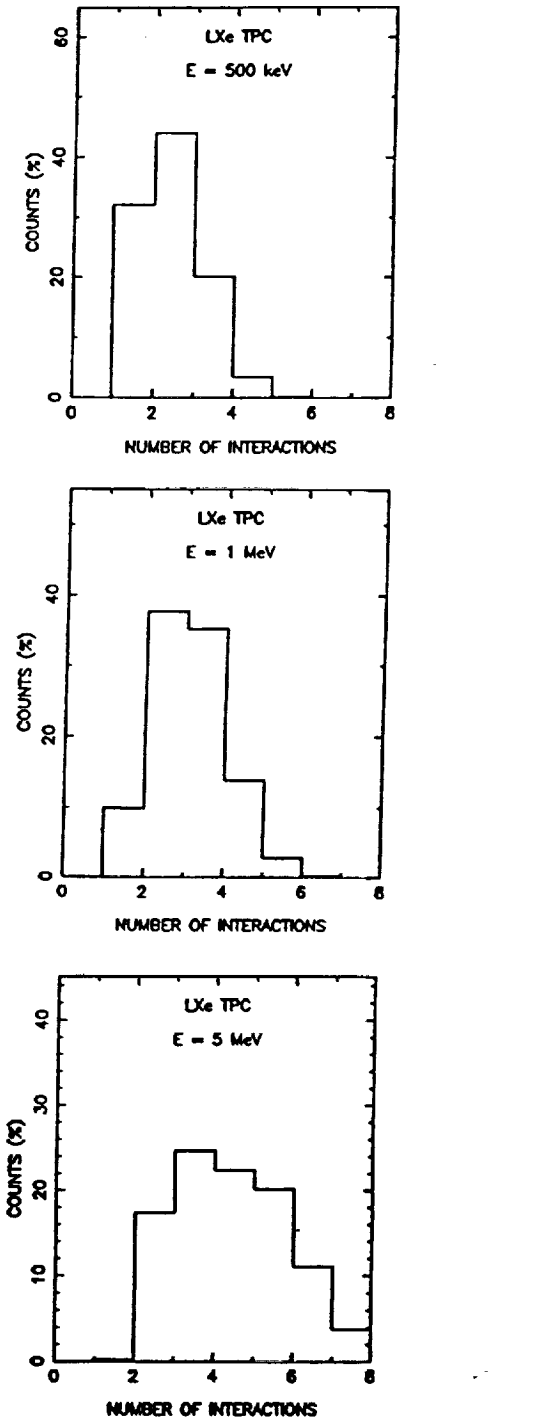

Fig. 2. Distribution of interaction points for γ-ray energies of 500 keV, 1 MeV and 5 MeV.

first interaction point is a Compton scattering is 90% at 1 MeV, decreasing to about 25% at 10 MeV. To improve the signal/noise level in the few MeV region where multiple Compton events dominate, an algorithm based on the kinematics of the Compton process was developed and tested. The algorithm uses the capability of the LXe-TPC to visualize each incoming γ-ray event and to reconstruct the initial direction from the energy deposited in each interaction point and the coordinates of the points. Consider an event in which a γ-ray produces N energy deposition points. Let W_0 be the energy of the incoming photon, W_i the energy of the scattered photon, E_i the energy of the scattered electron and $\cos\theta_i$ the cosine of the scattering angle. If the coordinates and the energy depositions for each interaction point, as well as the right order of the successive interactions are known, then from energy and momentum conservation we can write for each interaction point:

$$1 - \cos\theta_i = \frac{1}{W_i} - \frac{1}{W_{i-1}} \qquad (1)$$

where $W_i = W_{i+1} + E_{i+1}$, for $i = 1, N-1$. For any given distribution of interaction points generated inside the sensitive volume, we now assume that the last interaction point is a photo-absorption and that the initial direction of the incoming γ-ray is known. Calling

$$\frac{E_i}{1 - \cos\theta_i} = \alpha_i, \qquad (2)$$

(1) becomes

$$W_{i-1} \cdot W_i = \alpha_i. \qquad (3)$$

Similarly, for the $(i+1)^{th}$ point,

$$W_i \cdot W_{i+1} = \alpha_{i+1} \qquad (4)$$

From (3) and (4),

$$W_i = \frac{\alpha_i - \alpha_{i+1}}{E_i + E_{i+1}} \qquad (5)$$

Also, if the total energy is contained, W_0 is

$$W_0 = \frac{\alpha_1}{E_2 + E_3 + \cdots E_N} \qquad (6)$$

Alternatively, from energy conservation alone we have an independent estimate of the energy of the scattered photon at each point. We express this as W_i'.

$$W_i' = E_{i+1} + \cdots E_N \qquad (7)$$

for $i = 0, N-1$. To test the validity of the assumption that the total energy is contained, as well as if the assumed initial direction of the γ-ray is kinematically possible, the function

$$f = \sum_{i=0}^{N-1} (W_i - W_i')^2. \qquad (8)$$

is minimized for all possible combination of points. The calculation takes into account the errors on the energy and spatial coordinates.

2.3 Detection Efficiency

The Monte Carlo calculations were based on the EGS4 computer code [9]. The excellent gamma-ray detection efficiency of liquid xenon over a wide energy range is shown in Fig.3. The full energy peak efficiency was calculated for gamma-rays in the range 0.3-10 MeV, normally incident on the forward face of a 10 cm deep liquid xenon detector. The energy of the events in the sample was required to be totally contained. The use of a coded mask

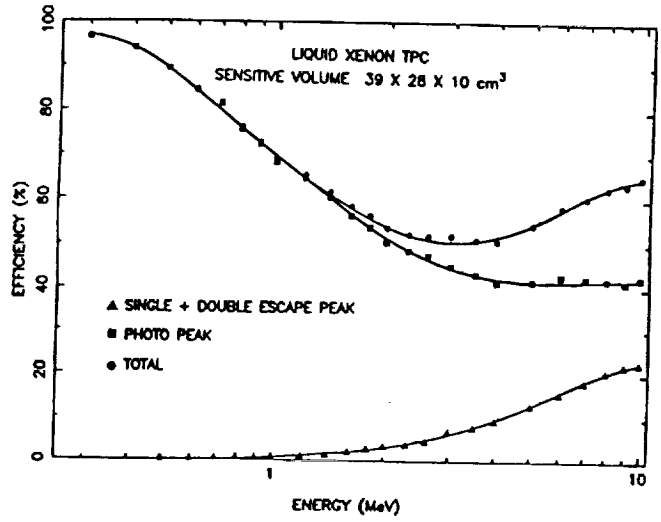

Fig. 3. Efficiency of the LXe-TPC for normally incident photons.

reduces the detection efficiency by a factor of two, assuming 100% opacity of the closed mask elements. This is shown in the upper curve of Fig. 4. The effect of 3 mm stainless steel detector wall was also accounted for. The effect of the Compton reconstruction algorithm, described in section 2.2, on the telescope efficiency is also shown in Fig. 4 with the points □. Because the algorithm is tailored for events which start with a Compton scattering, all events with a single photo-absorption or which start with a pair production are rejected. To recover the detection

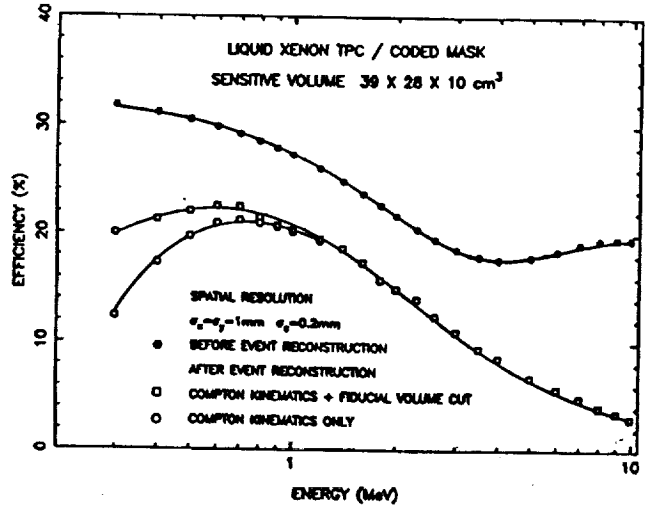

Fig. 4. Efficiency of the LXe-TPC/coded mask, before and after event reconstruction.

efficiency at low and high energy, different reconstruction techniques can be applied. For example, the majority of low energy photons coming from the source will interact in the top region of the LXe-TPC. Fiducial volume cuts for single site events can therefore drastically improve the signal/noise ratio. This is shown in Fig. 4 with the points •. All single-site events reconstructed outside the first 1 cm layer of liquid xenon from the top were rejected. For high energy events which start with a pair production, tracking of the electron/positron can be used, on an event-by-event basis, to estimate the γ-ray direction from the opening angle of the pair. Such an algorithm has however not been applied as one can see from the drastic drop in efficiency at energies above $\sim$ 2 MeV.

The capability of the reconstruction algorithm to reject events under the Compton continuum is shown in Fig. 5, which shows the ratio of the total counts under the peak to that under the Compton continuum. A large improvement in this ratio is achieved for the MeV region. The excellent capability of the same algorithm to recognize γ-ray events entering the TPC normally from the bottom was also tested. Results are shown in Fig. 6. For this calculation total energy containment was not required.

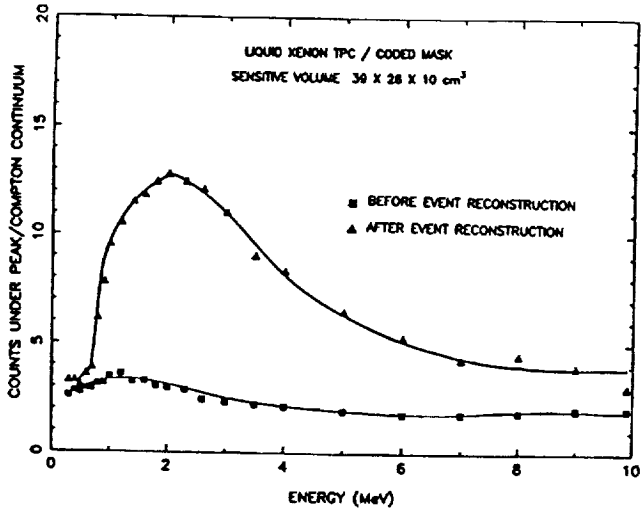

Fig. 5. Ratio of events under the peak to that under the Compton continuum for the LXe-TPC/coded mask before and after event reconstruction.

2.4 Background Reduction and Flux Sensitivity.

The ultimate flux sensitivity is perhaps the most relevant "figure-of-merit" of a γ-ray telescope. Among the factors which determine the sensitivity are: (i) the energy of the γ-rays and (ii) the detector's effective area, energy and spatial resolution, the exposure time and the total background rate. To calculate the background expected in the LXe-TPC/coded mask telescope at balloon altitudes, we have taken into account the dominant atmospheric and cosmic diffuse components, entering the forward aperture of the telescope or leaking through a thick (5 cm) CsI active shield. The flux and angular distribution of the atmospheric γ-rays used in the calculation were taken from the parameterized forms given by Costa et al. [10] and the cosmic diffuse spectrum used was that given in reference [11]. The internal backgrounds from natural radioactivity, cosmic ray induced radioactivity and activation of instrument materials has been neglected, as we expect to reject the majority of these single site events. Pulse shape

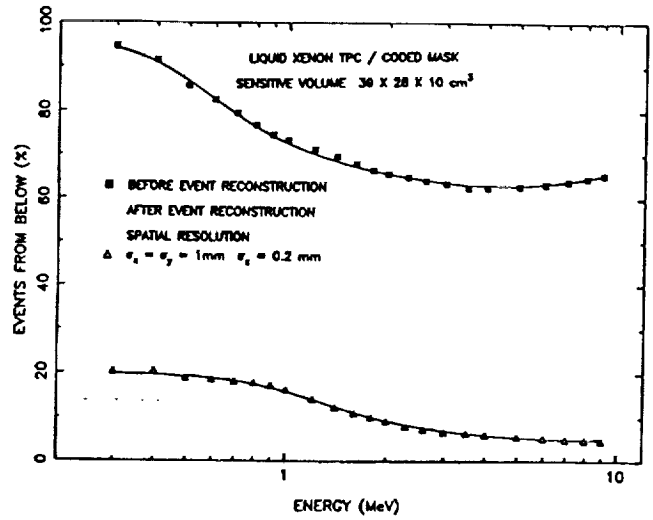

Fig. 6. Percentage of events entering the LXe-TPC from the bottom before and after event reconstruction.

discrimination of the scintillation light pulses offers additional background rejection capability, as it is strongly dependent on the ionization density of the event. For example, neutron induced events can easily be discriminated against, based on the light signature. Figure 7 shows the calculated background flux, before and after applying the Compton event reconstruction of section 2.2 and the fiducial volume cut. We assumed a float altitude of 3 g/cm^2, over Palestine, Texas. The integrated flux over the 0.1–10 MeV region gives about 340 counts/sec, consistent with typical background rates measured at these altitudes. A background reduction of almost a factor of 10 is obtained by identifying gamma-rays which kinematically couldn't have come through the FOV of the telescope. It is clear that even better background suppression can be achieved,

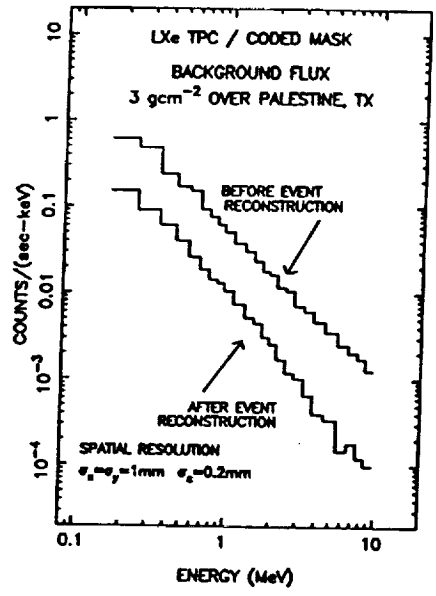

Fig. 7. Calculated background count rate before and after event reconstruction.

on an event-by-event basis, using different algorithms for different gamma-ray energies, as previously discussed.

From the calculated efficiency and background rate we have estimated the 3σ minimum flux sensitivity of the proposed telescope. The results are shown in Fig. 8a and 8b. For a typical exposure of 3×10^4s, we find a value of 9×10^{-5} photons/cm^{2}sec for 511 keV and of 6×10^{-5} photons/cm^{2}sec for 1.8 MeV. A continuum sensitivity of 3×10^{-7} photons/cm^{2}sec is obtained at 1 MeV. The sensitivity curves of the other instruments, shown for comparison, have been taken from Winkler (1991) [12]. When combined with the arcminute source localization accuracy, the high sensitivity of the LXe-TPC telescope makes it competitive with many satellite instruments, even with the much shorter observation time available in a ballloon flight.

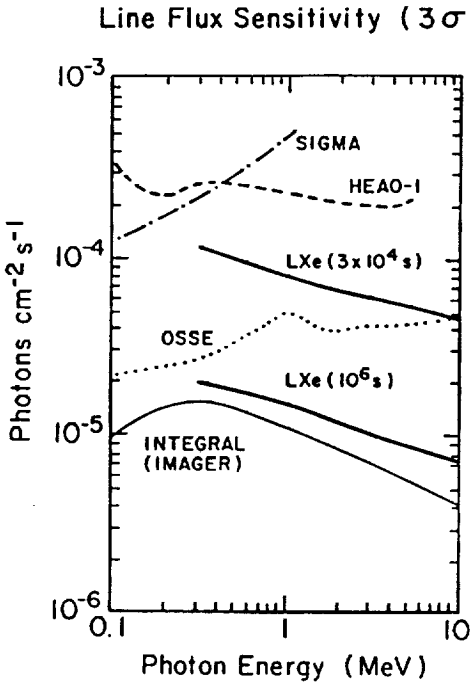

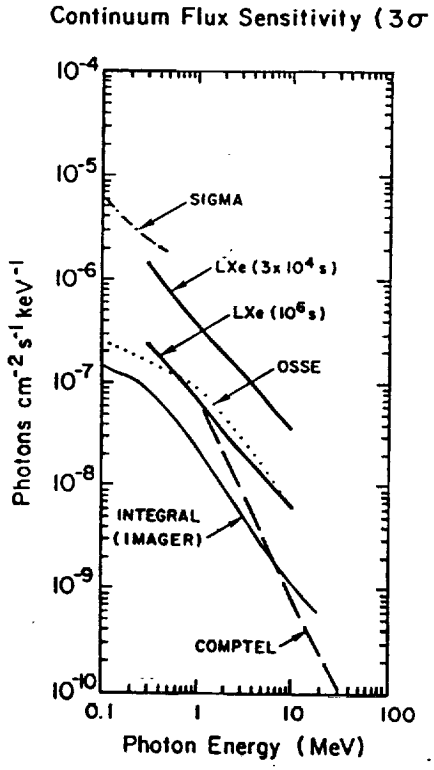

Fig. 8. The 3σ minimum (a) line and (b) continuum flux sensitivity of the LXe-TPC/coded mask γ-ray telescope.

4.CONCLUSION

Monte Carlo modeling of a realistic LXe-TPC/coded mask telescope has demonstrated the unique capability of this instrument to suppress background events as a direct consequence of the imaging properties of the LXe-TPC. By using a reconstruction algorithm for multiple site events, based on the kinematics of Compton scattering, we find that the expected background flux at balloon altitude is reduced by nearly an order of magnitude, resulting in superior line flux sensitivity in the MeV region, compared to that of existing scintillator-coded mask or proposed segmented germanium/coded mask γ-ray telescopes. It is clear that this is only a first step towards the application of the liquid xenon technique for precise imaging of cosmic γ-ray sources. The full potential will be realized when a detector with large effective area, improved energy resolution and sub-millimeter spatial resolution becomes practically operational as a Compton/pair production γ-ray telescope.

This work was supported by NASA grant NAGW-2013.

REFERENCES

[1] E. Aprile, R. Mukherjee and M. Suzuki, EUV, X-Ray and Gamma-Ray Instrumentation for Astronomy and Atomic Physics, SPIE Conference Proceedings, ed. C.J. Hailey and O.H.W. Siegmund, **1159** (1989) 295.

[2] P.P. Dunphy et al., Nucl. Instr. and Meth. **A274** (1989) 362.

[3] W.E. Althouse et al., Proc. 20th Int. Cosmic Ray Conf. 1 (1987) 84.

[4] J. Paul et al., Cospar Proc. on "Recent result and perspective instrumental developments in X and gamma-ray astronomy", Adv. Space Res. **11** No. 8 (1991) 289.

[5] E. Aprile et al., Nucl. Instr. and Meth. **A316** (1992) 29

[6] Prof. E. Chupp, Univ. of New Hampshire, private communications (1992).

[7] E. Aprile, R. Mukherjee and M. Suzuki, Nucl. Instr. and Meth. **A302** (1991) 177.

[8] E.E. Fenimore and T.M. Cannon, Appl. Opt. **17**, (1978) 337.

[9] R.L. Ford and W.R. Nelson, The EGS4 Code System, SLAC-210 (1978).

[10] E. Costa et al., Astrophysics and Space Science **100** (1984) 165.

[11] V. Schönfelder, V. Graser and J. Daugherty, Astrophys. J. **217** (1977) 306.

[12] C. Winkler, "Gamma ray line astrophysics", AIP conference proc. 232 (1991) 483.

APPENDIX B

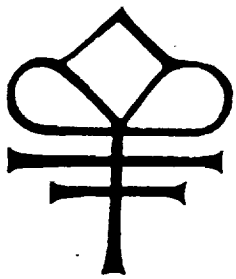

A Liquid Xenon Imaging Telescope for Gamma-Ray Astrophysics: Design and Expected Performance

E. Aprile, R. Mukherjee, D. Chen and A. Bolotnikov
Physics Department and
Columbia Astrophysics Laboratory, Columbia University
538 West 120th Street, New York, NY 10027, USA

Presented at the: 3rd *International Conference on Advanced Technology and Particle Physics,* Como, Italy, 22 – 26 June, 1992
To be published in: *Nuclear Physics B (Proc. Suppl.)*

COLUMBIA UNIVERSITY

DEPARTMENTS OF

PHYSICS and ASTRONOMY

NEW YORK, NEW YORK 10027

Columbia Astrophysics Laboratory Contribution Number 506

A Liquid Xenon Imaging Telescope for Gamma-Ray Astrophysics: Design and Expected Performance

E. Aprile, R. Mukherjee, D. Chen, and A. Bolotnikov

Physics Department and Columbia Astrophysics Laboratory
Columbia University, New York, NY 10027

A high resolution telescope for imaging cosmic γ-ray sources in the MeV region, with an angular resolution better than 0.5° is being developed as balloon-borne payload. The instrument consists of a 3-D liquid xenon TPC as γ-ray detector, coupled with a coded aperture at a distance of 1 meter. A study of the actual source distribution of the 1.809 MeV line from the decay of ^{26}Al and the 511 keV positron-electron annihiliation line is among the scientific objectives, along with a search for new γ-ray sources. The telescope design parameters and expected minimum flux sensitivity to line and continuum radiation are presented. The unique capability of the LXe-TPC as a Compton Polarimeter is also discussed.

1. INTRODUCTION

Gamma-ray telescopes with true imaging capability and high flux sensitivity are essential for studying the highest-energy phenomena in the universe. Fine imaging provides accurate positioning of the sources detected within the FOV and good angular resolution to map regions of diffuse emission and separate point source contributions. The importance of true source imaging is particularly evident in the study of two of the most pressing problems in low energy γ-ray astronomy: the 1.089 MeV line emission from the decay of ^{26}Al and the 511 keV positron-electron annihilation line emission from the Galactic Center.

In 1977, Ramaty and Lingenfelter [1] suggested that galactic nucleo-synthetic production of ^{26}Al in supernova events over the past few million years could give rise to a detectable γ-ray line at 1.809 MeV. This line arises from the electron capture (18%) or positron decay (82%) of the million-year mean life ^{26}Al and was first detected in 1984 [2] at a flux level of $4.3\pm0.8 \times 10^{-4}$ photons cm^{-2} s^{-1} rad^{-1} at the Galactic Center. Several subsequent confirmations of the line energy and flux level have been made. Some potential sources of ^{26}Al, which have been proposed, are supernovae, novae, red giants in the Asymptotic Giant Branch (AGB), Wolf-Rayet stars or nearby OB stars (see e.g., [3] for a recent review). Since these objects have more or less known or inferred galactic distributions, it is believed that a measurement of the spatial distribution of the ^{26}Al 1.809 MeV line intensity will identify the ^{26}Al source. The only instrument which could measure this radiation with imaging capability, is the Compton telescope, the most advanced version of which is COMPTEL on the *COMPTON* Observatory. COMPTEL however cannot directly measure the 1.809 MeV spatial distribution. The only definite statement that can be made about the ^{26}Al spatial distribution from the latest COMPTEL results, at the present time, is that a point source near the Galactic Center can be excluded [4]. Clearly, there is a requirement to measure directly the spatial distribution of the 1.809 MeV line with a true imaging telescope.

As for the 511 keV line, the debate between point like and diffuse nature of the emission continues to date and can only be fully resolved with a high level imaging map of the Galactic Center region at γ-ray energies.

At the present time the OSSE instrument on the *COMPTON* Observatory is mapping the distribution of the annihilation line [5]. Since the OSSE measurements give the lowest galactic center flux measurements so far Skibo, Ramaty and Leventhal [6] have used these results

and other off-center measurements to test different models for the origin of the diffuse or steady galactic plane 511 keV component. On the other hand, the origin of the variable narrow line galactic 511 keV radiation may be associated with the bright hard X-ray source 1E1740.7-2942 which was studied by the imaging telescope SIGMA on the *GRANAT* satellite during the spring-fall of 1990 and in early 1991. Sunyaev *et al.* [7] have identified three spectral states for this source which range from a "low state," a normal (Cygnus X–1 like) state to a hard state in which a bump appears in the spectrum between (300–600) keV. The broad feature of the spectrum has been interpreted as annihilation of positrons in a hot medium ($\sim$ 40 keV). This is consistent with the temperature of the accretion disk derived from the X-ray continuum spectrum.

Subsequently it was proposed [8,9] that in addition this high energy source injects positrons into a molecular cloud where they slow down and annihilate to produce the narrow component of the 511 keV line emission.

Future studies of the 511 keV emission require the most advanced imaging telescope with good to excellent energy resolution.

Of the techniques proposed for γ-ray imaging and spectroscopy of astrophysical sources, the Liquid Xenon Time Projection Chamber (LXe-TPC) is among the most promising. The properties of liquid xenon make it very efficient for γ-ray detection. When used in an ionization chamber, operated in the time projection mode, this medium offers a combination of high detection efficiency, excellent spatial resolution and very good energy resolution. Like an electronic bubble chamber, a LXe-TPC with three-dimensional position sensitivity is capable of visualizing the complex histories of γ-ray events initiated by either Compton scattering or pair-production. As a result, efficient background rejection is also achieved, reducing the requirement for massive anticoincidence shielding of the type that is required for germanium or sodium iodide γ-ray detectors. The angular resolution of the LXe-TPC as a Compton telescope is however limited, in the few MeV region, by the small separation between two successive γ-ray interactions [13]. To achieve imaging with good angular resolution at low energies, the combination of the imaging LXe-TPC with a coded aperture is proposed.

A unique consequence of the LXe-TPC imaging capability is its sensitivity as a Compton polarimeter. Besides the precise determination of the energy and incident direction of a photon, determination of its polarization state can give further information on the source of γ rays. The main production mechanisms which can give polarized γ rays are: bremsstrahlung from electron beams, electron synchrotron radiation, electron curvature radiation, and γ rays from deexcitation of nuclei excited by directed ion beams. In the case of the Crab Nebula it has been determined that the nebular X-ray emission is polarized [10]. Existence of UHE ($> 10^{14}$) electrons in this source could yield polarized nebular γ-rays of a few MeV. If curvature radiation from electrons is the source of MeV γ rays in pulsars, such as the Crab and Vela, then polarization might also be expected.

In general it has been recognized in the study of X-ray sources, that measurement of the direction and magnitude of the photon polarization could significantly contribute to a better understanding of the physical processes in compact objects, such as pulsars, Black Holes and AGN.

2. TELESCOPE DESIGN

2.1. Introduction

The telescope is schematically shown in Fig. 1. It consists of a coded aperture mask, located 1 meter above a LXe-TPC. The sensitive area of the TPC is 39 x 28 cm^2. The active depth of liquid xenon is 10 cm. Fig. 2 shows the LXe-TPC in more detail. The event trigger to the readout electronics is provided by the fast primary scintillation light detected by two UV sensitive PMTs. The intrinsic instrumental angular resolution in the coded mask configuration is determined by the size of the mask unit cell, the mask-detector separation, and by the accuracy to which the photon interaction points in the detection plane can be determined. The coded mask that we have assumed in our design and Monte Carlo simulations consists of a 85 x 83 element pattern of

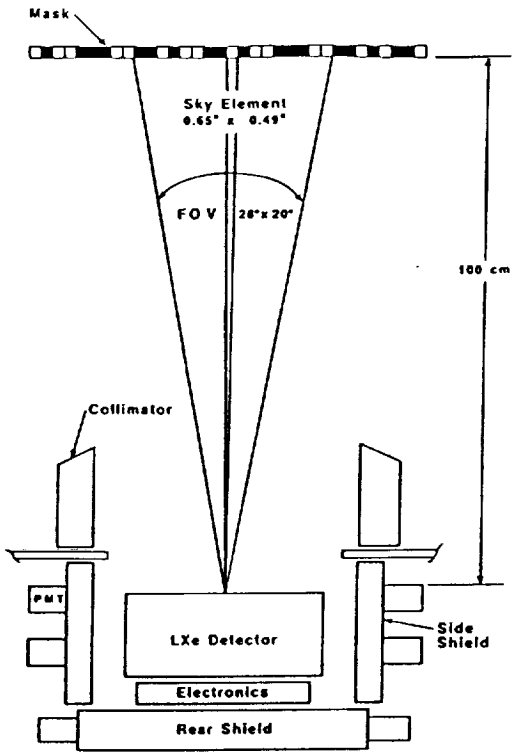

Energy Range	0.3-10 MeV
Energy Resolution	4.5% FWHM at 1 MeV
Spatial resolution	1 mm
Geometrical area	1200 cm^2
FOV (Fully Coded)	28° × 20° FWHM
Angular resolution	30′
Point source location accuracy	1′ (10σ source)
Min Flux (Line) 3σ at 1 MeV	8×10^{-5} ph $cm^{-2}s^{-1}$ (3×10^4s)
Min Flux (Continuum) 3σ at 1 MeV	3×10^{-7} ph $cm^{-2}s^{-1}keV^{-1}$ (3×10^4s)

Fig. 1. Schematic of the LXe-TPC/coded mask imaging γ-ray telescope.

$0.91 \times 0.58 \times 1.2$ cm^3 thick blocks of tungsten alloy. The 1 meter separation between the mask and the LXe detector plane is determined by the University of New Hampshire gondola [11] which we plan to use for the first balloon flight. This defines a pixel element of angular dimension 0.65° × 0.49°. The nominal FOV is 28° × 20°

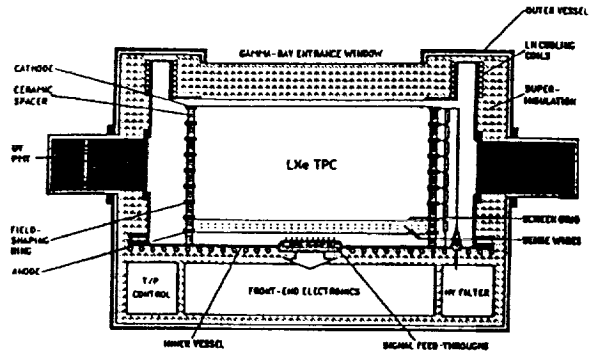

Fig. 2. Schematic of the LXe-TPC detector.

and the source localization accuracy is estimated to be $\sim$ 1 arcminute, for a 10σ source strength. For background suppression at balloon altitude an active shield has been assumed around the detector. The type and amount of shield needed will ultimately be determined by the type of event triggering and selection on board, by dead time consideration, telemetry rate as well as cost and weight consideration.

2.2. The LXe-TPC: Status of Development

A LXe-TPC works on the principle that free ionization electrons liberated by a charged particle in the liquid can drift, under a uniform electric field, from their point of creation towards a signal read-out region. Here the charge signals induced or collected on sensing electrodes are detected to yield both the spatial distribution of the ionizing event and its energy.

For γ-rays it is the electrons or positrons created by photoabsorption, Compton scattering or pair production, which will ionize as well as excite the xenon atoms creating a large number of electron-ion pairs and scintillation photons. For 3-D imaging of γ-ray events in LXe we plan to use a sensing electrodes geometry based on the original design by Gatti *et al.* [12]. Two orthogonal induction wire planes separated from the drift region by a screening grid, give the X-Y event information. The measured drift time, referred to the scintillation trigger, and the known drift velocity provides the Z-information. The total event energy is measured from the total charge collected on an anode plate, placed below the induction

wires.

In order to verify the feasibility of such a detector, the Columbia group started in 1989 an intensive R&D program on LXe. The attenuation length of electrons and UV photons in purified liquid xenon, the ionization and scintillations yields of electrons and alpha particles, the energy and spatial resolution have been studied.

The experimental results obtained on these aspects relevant for the development of a liquid ionization TPC, are documented in several references [13-18]. Especially relevant are the latest experimental results obtained with a 3.5 liter 2D-TPC prototype [19] equipped with a multi-wire structure to detect the induction signals in liquid xenon. The results demonstrate both the capability of a large volume LXe detector to provide similar or better energy resolution than the previously reported value of 4.5% FWHM for 1 MeV radiation, as well as the imaging capability.

Figure 3 shows an example of collection and induction signals produced by a γ-ray event in the LXe-TPC prototype. The induction signal, which has the expected triangular shape, has a large S/N ratio of 12:1, even for a typical point-like charge deposition produced by a γ-ray interaction. The dependence of the induced signal on the lateral position of the drifting electron cloud

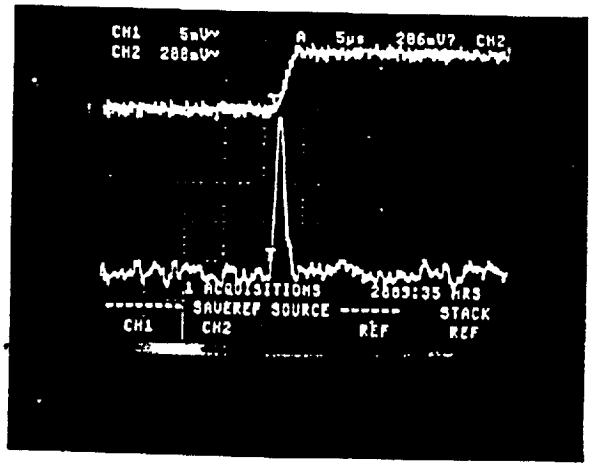

Fig. 3. Collection signal (upper trace Gain=1) and induction signal (lower trace Gain=400) produced by a γ-ray event in the 3.5 liter LXe-TPC prototype.

with respect to the wire cell [19], offers the possibility to derive the spatial coordinate of each event by weighting the signal amplitude on neighbouring wires. Thus the spatial resolution in the X-Y plane, can be better than $s/\sqrt{12}$, where s is the wire spacing.

Experimental work on the operation and performance of the LXe TPC prototype implemented for full 3-D imaging and triggered by the scintillation light is in progress.

3. TELESCOPE PERFORMANCE: MONTE CARLO RESULTS

3.1. Background Rate and Minimum Flux Sensitivity.

To calculate the background expected in the LXe-TPC/coded mask telescope at balloon altitudes, we have taken into account the dominant atmospheric and cosmic diffuse components, entering the forward aperture of the telescope or leaking through the active shield (5 cm thick CsI). The flux and angular distribution of the atmospheric γ-rays used in the calculation were taken from the parameterized forms given by Costa *et al.* [20] and the cosmic diffuse spectrum used was that given by Shonfelder, Graser and Daugherty [21]. The internal backgrounds from natural radioactivity, cosmic ray induced radioactivity and activation of instrument materials have been neglected, as the majority of these single site events can be rejected by simple fiducial volume cuts.

The results of the calculation are shown in Fig. 4. The integrated flux over the 0.1–10 MeV region gives about 340 counts/sec, consistent with typical background rates measured at the assumed altitude. An event reconstruction algorithm based on the kinematics of Compton scattering was developed and used for identification and rejection of background events [22]. As shown in Fig. 4, a background reduction of approximately a factor of 10 is obtained by identifying γ-rays which kinematically couldn't have come through the FOV of the telescope, and by applying a fiducial volume cut to remove low energy events.

Based on the calculated γ-ray detection efficiency [22] and the calculated background rate,

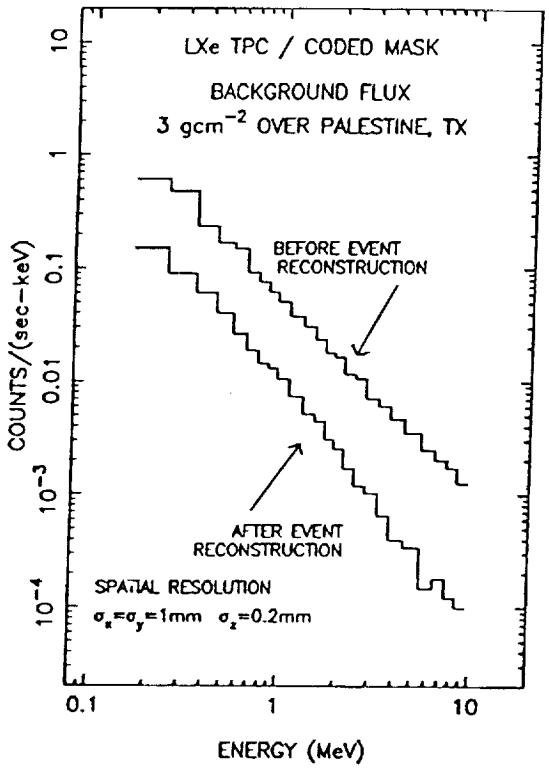

Fig. 4. Monte Carlo calculation of the background flux at balloon altitude.

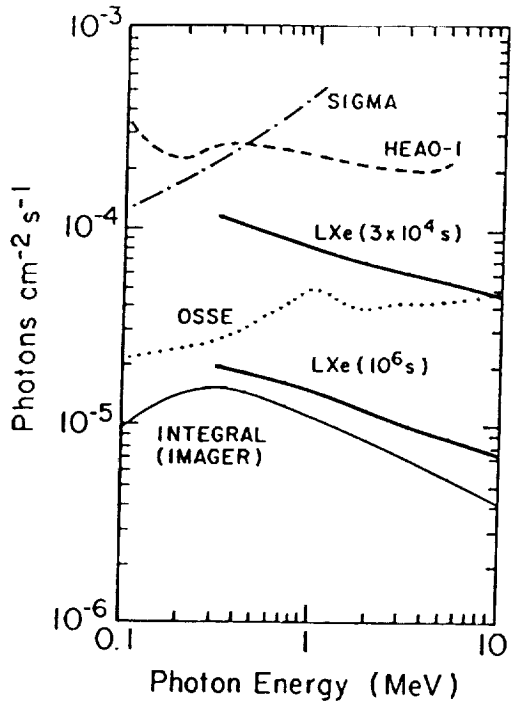

Fig. 5. 3σ minimum line flux sensitivity of the LXe-TPC/coded mask γ-ray telescope.

we have obtained the 3σ minimum flux sensitivity shown in Fig. 5. With a typical balloon flight exposure of 3×10^4s, the 3σ line sensitivity is 6×10^{-5} photons cm^{-2} s^{-1} (1.8 MeV line) and 9×10^{-5} photons cm^{-2} s^{-1} (511 keV line). The continuum sensitivity is 3×10^{-7} photons cm^{-2} s^{-1} keV^{-1} at 1 MeV. The sensitivity curves of the instruments, shown for comparison, have been taken from Winkler [23]. When combined with the excellent source localization accuracy, the high sensitivity of the LXe-TPC telescope makes it competitive with many satellite instruments, even with the much shorter observation time available in a balloon flight.

3.2. Simulated Observations of the Crab and 511 keV Line

The Crab Nebula/Pulsar will be the primary target for the first verification balloon flight of the LXe-TPC coded mask γ-ray telescope. This source is one of the most intense in our energy range and is stable, both in intensity and spectrum. Monte Carlo simulations of the expected Crab signal were performed using the complete telescope system shown in Fig. 1.

The Crab Nebula was assumed to be a point source in the sky with a spectrum equal to 5.5×10^{-4} (E/100 keV)$^{-2.2}$ photons cm^{-2} s^{-1} keV^{-1} at 10 MeV [24]. The source was aligned with the telescope axis and the observing time was 10^4 s. The estimated background of Fig. 4, after event reconstruction, was uniformly distributed in the detector's plane and added to the shadowgram of the source. Figure 6 shows the resulting deconvolved image of the Crab, for the energy interval 0.3 – 0.5 MeV. The Crab signal dominates over the background up to several MeV with a S/N of about 20σ.

Simulated observations have also been performed for the low and high state of the 511 keV Galactic Center annihilation line. A 10^4 s exposure time was assumed. The source was placed in the center of the FOV, and superimposed on

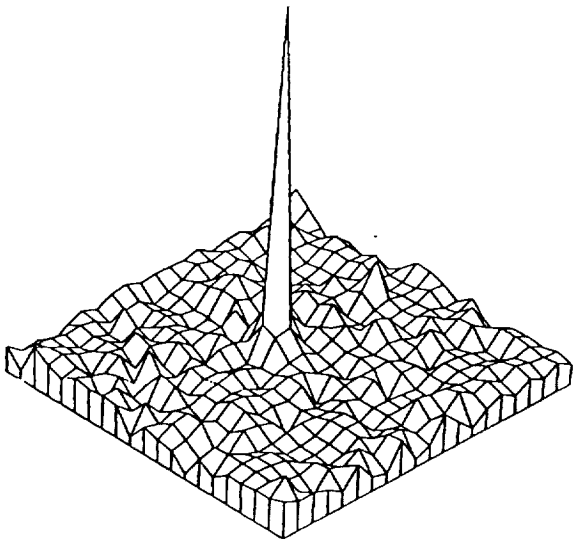

Fig. 6. Monte Carlo simulation of the Crab as a point γ-ray source in the energy range (0.3–0.5 MeV).

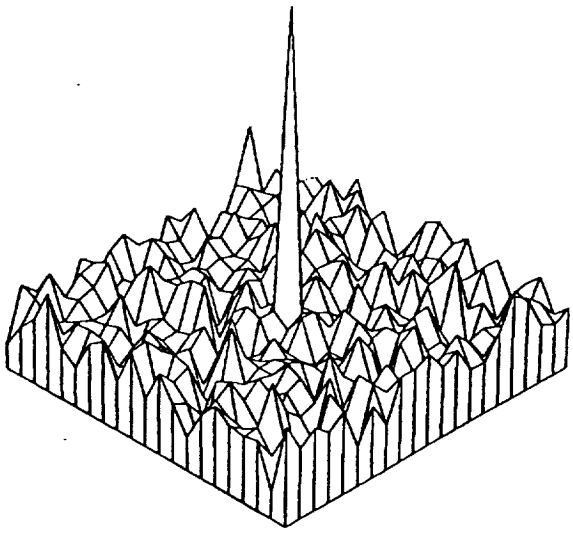

Fig. 7. Monte Carlo simulation of the 511 keV Galactic Center point source observed for High State.

a uniformly distributed background of 4×10^{-2} counts s^{-1} keV^{-1}, as from our estimate. The intensity of the 511 keV line source was chosen to be 2×10^{-4} photons cm^{-2} s^{-1} for the "low state" and 1×10^{-3} photons cm^{-2} s^{-1} for the "high state".

Figure 7 shows the result of the 511 keV image for the "high state". Even in the "low state", the 511 keV flux can be detected by our instrument at a satisfactory significance level of $\sim 4\sigma$.

3.3. Polarization Sensitivity

The LXe-TPC imaging capability is also ideal to measure the linear polarization of the incident γ-ray undergoing Compton scattering. The linear polarization of γ-rays can be measured based on the principle that the Compton scattering process is sensitive to the polarization of the incident γ-ray, the cross-section for Compton scattering being the largest for the case when the direction of the scattered γ-ray is normal to the polarization vector of the incident γ-ray. The advantage of a LXe-TPC Compton Polarimeter over the conventional NaI(Tl), CsI(Tl) or Ge(Li) double scatter Compton telescopes is the enhanced detection efficiency offered by a single detector working both as scatterer and absorber, as well as its combination of good energy and position sensitivity.

A Monte Carlo program was developed to estimate the polarization sensitivity of the LXe-TPC for a 100% polarized γ-ray beam of energy varying from 300 keV to 4 MeV, incident normally on the detector surface. Figure 8 shows the result. For comparison, the polarization sen-

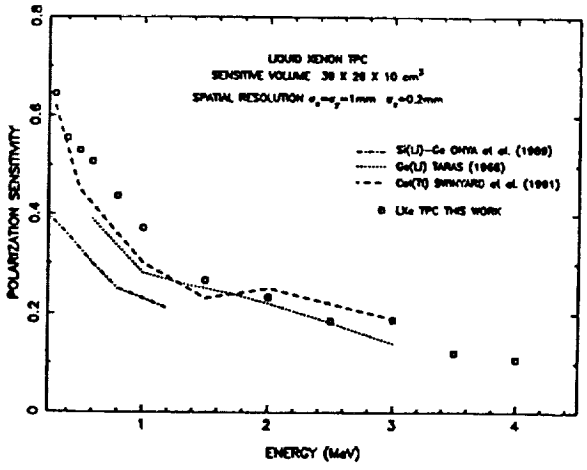

Fig. 8. Monte Carlo calculation of the LXe-TPC polarization sensitivity.

sitivity of the Ge(Li) polarimeter [25], the Si(Li) [26] and the CsI(Tl) polarimeter of the Imager on INTEGRAL [27] are also shown. The unique feature of the LXe-TPC is its capability to infer the scattering angle θ and the azimuthal angle ϕ, with an accuracy of about 0.5° [13], for each scattered γ-ray. We can thus obtain the azimuthal angular distribution of the scattered γ-rays by selecting events from different intervals of scattering angle. By applying the detector's response function, calculated or measured during calibration tests with polarized beams, we can deconvolute the original γ-ray polarization. Figure 9 shows the modulation curve in the range $\phi = 0°$ to $\phi = 90°$, simulated for 100% polarized γ-rays of energy 500 keV.

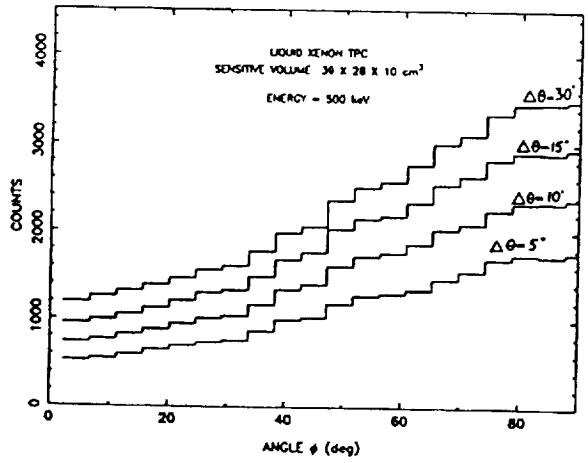

Fig. 9. Modulation curve of the LXe-TPC for 100% polarized γ-rays of energy 500 keV.

4. CONCLUSION

The design and expected performance of a γ-ray imaging telescope tailored to the 0.3–10 MeV energy region have been discussed. The telescope combines the excellent properties of a liquid xenon TPC as 3-D position sensitive γ-ray detector with the well established imaging properties of a coded aperture mask, to achieve high efficiency, good spectroscopy and angular resolution over the entire energy range of interest. The high sensitivity to MeV γ-ray lines and continuum complemented with the good imaging capability will permit the observation of a variety of astrophysical sources. Important contributions to the field of low energy astrophysics as well as new discoveries are expected even in the maiden balloon flight which is planned for the end of 1994.

This work was supported by NASA (Award NAGW 2013).

5. REFERENCES

[1] R. Ramaty, and R.E. Lingenfelter, *Ap.J. (Letters)*, 213, L5 (1977).

[2] W.A. Mahoney *et al.*, *Ap.J.*, 286, 578 (1984).

[3] N. Prantzos, *Astron. Astrophys. Suppl.*, in press (1992).

[4] R. Diehl *et al.*, *Astron. Astrophys. Suppl.*, in press (1992).

[5] W.A. Purcell, *et al.* in *The Compton Observatory Science Workshop*, NASA Conf. Publ. 3137, eds. C.R. Shrader, N. Gehrels and B. Dennis, 43 (1992).

[6] J.G. Skibo, R. Ramaty, M. and Leventhal, *Ap.J.*, in press (1992).

[7] R. Sunyaev, *et al.*, *Ap. J. (Letters)*, 383, L49 (1991).

[8] J. Bally and M. Leventhal, *Nature*, 353, 234 (1991).

[9] I.F. Mirabel *et al.*, *Nature*, 358, 215 (1992).

[10] M.C. Weisskopf *et al.*, *Ap.J. (Letters)*, 220, L117 (1978).

[11] P.P. Dunphy *et al.*, *Nucl. Instr. and Meth.*, A274, 362 (1989).

[12] E. Gatti *et al.*, *Trans. Nucl. Sci.*, NS-26, 2910 (1970).

[13] E. Aprile, R. Mukherjee, and M. Suzuki, "EUV, X-Ray and Gamma-Ray Instrumentation for Astronomy and Atomic Physics," *SPIE Conference Proceedings*, ed. C.J. Hailey and O.H.W. Siegmund, 1159, 295 (1989).

[14] E. Aprile, R. Mukherjee, and M. Suzuki, *IEEE Trans. Nucl. Sci.*, NS-37, No. 2, 553 (1990).

[15] E. Aprile, R. Mukherjee, R. and M. Suzuki, *Nucl. Instr. and Meth.*, A302, 177 (1991).

[16] E. Aprile, R. Mukherjee, and M. Suzuki, *Nucl. Instr. and Meth.*, A300, 343 (1991).

[17] E. Aprile, R. Mukherjee, and M. Suzuki, *Nucl. Instr. and Meth.*, **A302**, 177 (1991)

[18] E. Aprile *et al.*, *Nucl. Instr. and Meth.*, **A316**, 29 (1992).

[19] E. Aprile *et al.*, accepted for publication in *SPIE proceedings* (1992).

[20] E. Costa, *et al.*, *Astrophysics and Space Science*, **100**, 165 (1984).

[21] V. Schönfelder, V. Graser, V. and J. Daugherty, *Ap.J.*, **217**, 306 (1977).

[22] E. Aprile *et al.*, accepted for publication in *Nucl. Instr. and Meth.* (1992).

[23] C. Winkler, *Gamma-Ray Line Astrophysics*, *AIP Conf. Proc.*, **232**, p. 483 (1991).

[24] J.C. Ling, and C.D. Dermer, *B.A.A.S.*, **22**, 1271 (1990).

[25] P. Taras, *Nucl. Instr. and Meth.*, **61**, 321 (1968).

[26] S. Ohya *et al.*, *Nucl. Instr. and Meth.*, **A276**, 223 (1989).

[27] B.M. Swinyard *et al.*, *SPIE*, Vol. 1548 *Production and Analysis of Polarized X-rays*, 94 (1992).

APPENDIX C

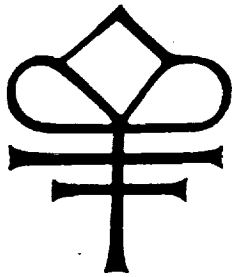

Liquid Xenon Time Projection Chamber for Gamma Rays in the MeV Region: Development Status

E. Aprile, A. Bolotnikov, D. Chen and R. Mukherjee
Department of Physics and
Columbia Astrophysics Laboratory, Columbia University
538 West 120th Street, New York, NY 10027, USA

Presented at the: *"Gamma-Ray Detectors"*
Conference of the SPIE's International Symposium
on Optical Engineering, 19 –24 July 1992

COLUMBIA UNIVERSITY

DEPARTMENTS OF

PHYSICS and ASTRONOMY

NEW YORK, NEW YORK 10027

Columbia Astrophysics Laboratory Contribution Number 500

Liquid Xenon Time Projection Chamber for Gamma Rays in the MeV Region: Development Status

E. Aprile, A. Bolotnikov, D. Chen and R. Mukherjee

Dept. of Physics and
Columbia Astrophysics Laboratory
Columbia University, New York NY 10027

ABSTRACT

The feasibility of a large volume Liquid Xenon Time Projection Chamber (LXe–TPC) for three-dimensional imaging and spectroscopy of cosmic gamma-ray sources, was tested with a 3.5 liter prototype. The observation of induction signals produced by MeV gamma-rays in liquid xenon is reported, with a good signal-to-noise ratio. The results represent the first experimental demonstration with a liquid xenon ionization chamber of a non-destructive read-out of the electron image produced by point-like charges, using a sense wire configuration of the type originally proposed in 1970 by Gatti et al. An energy resolution as good as that previously measured by us with millimeter size chambers, was achieved with the large prototype of 4.4 cm drift gap.

1. INTRODUCTION

Liquid xenon (LXe) is a very attractive medium for γ-ray detectors, because of its excellent combination of: high atomic number (Z=54), high density (3.06 gcm^{-3}), low W-value (15.6 eV), small Fano factor (0.04), small diffusion coefficient (65 cm^2s^{-1}), and high electron mobility (> 2000 $cm^2s^{-1}V^{-1}$). When used in an ionization chamber operated in the time projection mode (TPC), this medium combines high detection efficiency, excellent spatial resolution, very good energy resolution, and superior background identification and rejection ability. Thus, a LXe-TPC offers an unique potential for spectroscopy and imaging of cosmic γ-ray sources with high sensitivity and good angular resolution. The continuing emphasis of our research program has been to demonstrate the feasibility of high resolution liquid xenon imaging detectors in the field of γ-ray astrophysics. In the energy range from $\sim$ 100 keV to $\sim$ 30 MeV future advances require at least arcminute angular resolution and flux sensitivity for γ-ray lines (e.g. MeV) at the level of 10^{-6} photons cm^{-2} s^{-1}. Following these considerations, two γ-ray telescope designs based on a LXe-TPC tailored to a specific energy range and scientific program, emerged from our studies.

The first one is optimized for the few MeV energy region. It uses a LXe-TPC with 10 cm drift gap and 1200 cm^2 sensitive area, with millimeter spatial resolution requirement. By combining the 3-D position sensitive LXe γ-ray detector with a coded aperture mask at a separation of 1 meter, an angular resolution better than 0.5° can be achieved over the entire energy range 0.3–10 MeV. The unique capability of the LXe detector to use Compton kinematics to reject background events as well to measure polarization of MeV γ-rays with high sensitivity is emphasized for this version of a LXe-TPC telescope, which we plan to test in the near space environment as a balloon-borne payload. The study of two of the most pressing problems in low energy γ-ray astronomy, namely the determination of the actual source distribution of the 0.511 MeV positron-electron annihilation line and of the 1.809 MeV ^{26}Al line, will be the main scientific objective.[1,2]

The second telescope consists of a LXe-TPC with a larger sensitive volume (> 30 liters) and superior spatial resolution, optimized for the 1 – 30 MeV energy region where Compton scattering and pair production are the dominant γ-ray interaction processes. In a Compton telescope, the true direction of the γ-ray source can only be unambiguously identified when the direction of the Compton scattered electrons or electron-positron pairs are accurately measured. In the dense liquid xenon, the range of these electrons is very short (of the order of millimeters) so that a spatial resolution of a few hundred microns is required.[3]

There are many technical challenges to the construction of the LXe-TPC for these γ-ray telescopes. The most fundamental one is the purity of the liquid, which has to be at the ppb level to permit the drift of ionization electrons

over large distances. This problem has already been extensively studied and solved by us.[4] The second very important problem is the implementation of a non-destructive readout of the electronic signals to realize the 3-D imaging of any ionizing event in the sensitive volume. We report here, for the first time, the initial results from a study of the imaging performance of a 3.5 liter LXe-TPC as γ-ray detector. The equally important issue of good energy resolution in a large volume liquid xenon detector was also studied with this prototype and the results are presented here. These results are the first experimental evidence of the feasibility of a LXe detector of practical size and of its capability for good calorimetry and imaging.

2. LXe-TPC PROTOTYPE

The technical challenges of a liquid xenon detector for γ-rays were addressed with the development of a 3.5 liter prototype, shown schematically in Fig. 1. The detector is a large volume gridded ionization chamber with a maximum drift gap of 6.0 cm, compared to the 10 cm of the proposed LXe-TPC telescope. The active volume is defined by the cathode plate, the shielding grid and a sequence of equally spaced shaping rings which ensure the uniformity of the electric field for the drift of the electrons. The total active volume of ~ 365 cm^3 (7.8 cm $\times$ 7.8 cm $\times$ 6.0 cm), is much larger than the size of the typical liquid xenon ionization chambers reported in the literature so far. To irradiate the liquid xenon with γ-rays, a ^{207}Bi source is placed on the cathode plate, facing away from the active volume. Radiation entering the active volume has to first pass through 3 mm of stainless steel. This effectively blocks all conversion electrons from the ^{207}Bi so that the detector is sensitive only to γ-ray interactions.

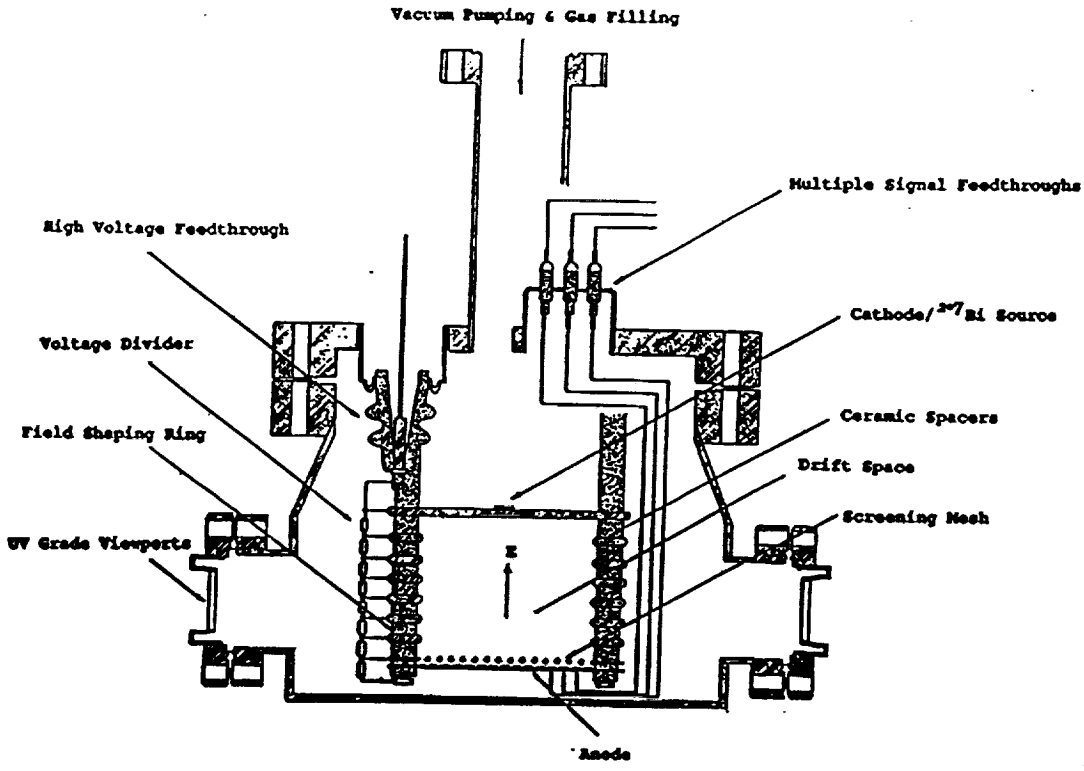

Fig. 1. The 3.5 liter LXe-TPC prototype γ-ray telescope.

To study the energy resolution, a single charge collector was placed 7 mm behind the shielding grid. The grid is actually a mesh made of nickel, with 0.8 mm spacing and 50 μm wire width spot-welded on a stainless steel frame. The field strengths on the two sides of the mesh have to be optimized to obtain a maximum shielding efficiency and transparency for the drifting electrons. The critical field ratio of 1.75, was calculated by the formula given by Bunemann et al.,[5] modified for a mesh type grid. This value was verified experimentally. During the operation of the detector a field ratio of 2 was typically chosen. A custom built low noise, charge sensitive preamplifier was used

to detect the signals from the collector plate. To allow the observations of slow rising signals, the decay time of the amplifier was set to 1 ms. To reduce the input capacitance, the amplifier was mounted as close as technically feasible to the signal feed-through.

To study the spatial resolution the chamber structure was modified into a 2-D TPC, with the electrode geometry shown schematically in Fig. 2. The same cathode plate with the radioactive source was used for these experiments. The shielding mesh was replaced by a plane of equally spaced wires with a pitch of 2 mm. Between this grid and the collector plate, a plane of sense wires, with the same 2 mm pitch, was introduced for the detection of the induction signals. The induction plane was at a distance of 2 mm from the shielding grid plane and 4 mm from the collector plate.

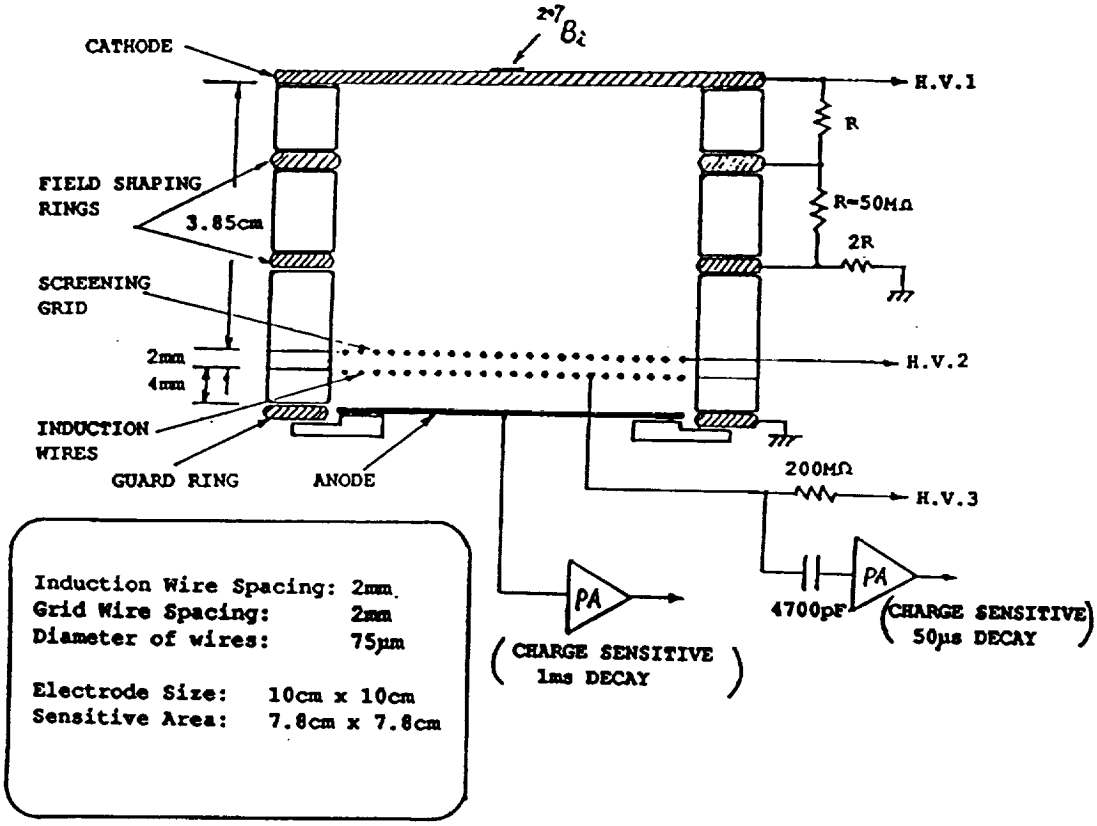

Fig. 2. Schematic of the 2-D LXe-TPC electrode structure for the measurement of the induction signals.

This electrode arrangement provides the two coordinates for the position of each point of interaction, one coordinate being determined by the drift time and the other by the position of the sense wire. For a non-destructive readout of the electron image on the induction wires, the electric field between the induction and the collection planes has to be correctly chosen so as to allow the field lines to pass between the sense wires. The right potentials for this condition were calculated and the field map is shown in Fig. 3.

The sense wires are biased with their "natural" potential in order not to distort the field distribution. The induction signal on each wire is detected with a low noise charge sensitive preamplifier, via a decoupling capacitor. Due to the fast rise time of these signals a decay time of 50 μs was used. The total number of sense wires read-out was 20. The output of each preamplifier was connected to a FADC through an additional amplification stage.

To purify the xenon gas needed to fill the 3.5 liter volume, we used the purification system shown in Fig. 4. This is essentially a larger scale version of the purification system previously used for liquid xenon chambers.

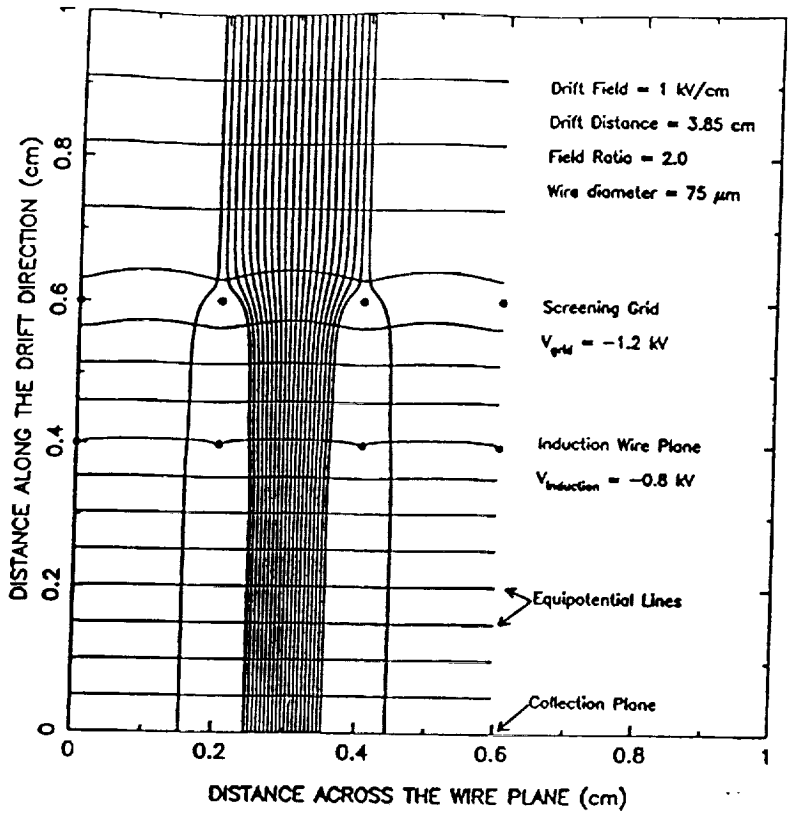

Fig. 3. The electric field map of the 2-D LXe TPC of Fig. 2.

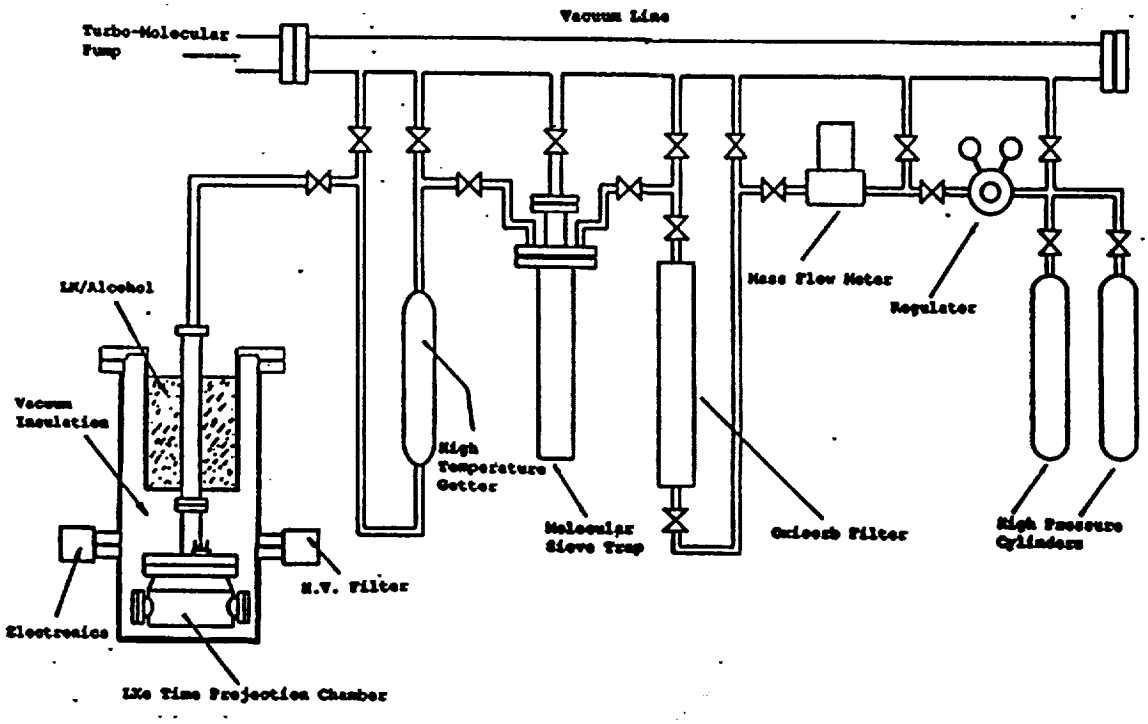

Fig. 4. The xenon gas purification system.

The system uses a combination of Oxisorb, cold molecular sieves, and high temperature getters, to effectively reduce electronegative impurities from commercial xenon gas, to less than 1 ppb. Details on the design and performance of our system can be found in an earlier publication.[4] To maintain the purity of the liquid, special care is paid in the preparation of the detector vessel and internal structure, as well as any other material in contact with the gas or the liquid. Pre-cooling of the xenon gas was achieved by surrounding a long filling pipe on top of the chamber vessel by a liquid nitrogen bath. Once the chamber vessel was full, an operating liquid temperature of about $-100°C$ was easily maintained by a mixture of liquid nitrogen and ethyl alcohol.

3. EXPERIMENTAL RESULTS

3.1. Energy Resolution Performance

Figure 5 shows the typical output signals of the charge sensitive preamplifier. The steps in the signals clearly indicate the different ionization processes, produced by the ^{207}Bi γ-ray interactions inside the LXe sensitive volume. For a gridded ionization chamber, the induced charge signal starts once the electrons pass the shielding mesh and linearly increases as the electrons move towards the collector. Since the decay time constant of the amplifier is much longer than the drift time, the pulse height appears to be constant after a step. The rise time of a single step is about 2.5 μs, which corresponds directly to the drift time between mesh and anode. This is consistent with the signal produced by a point like charge, as expected by the short range (much less than 1 mm) of low energy electrons in liquid xenon. This results in the unique feature of a liquid xenon ionization chamber to visualize the multiple-site energy depositions produced by the interactions of MeV γ-rays. Figure 5 clearly demonstrates this feature. The single step signal is due to a photoelectric interaction (Fig. 5 a). The multi-step signals are due to multiple-site interactions produced by one or more Compton scatterings followed by a photoelectric absorption (Fig. 5 b,c).

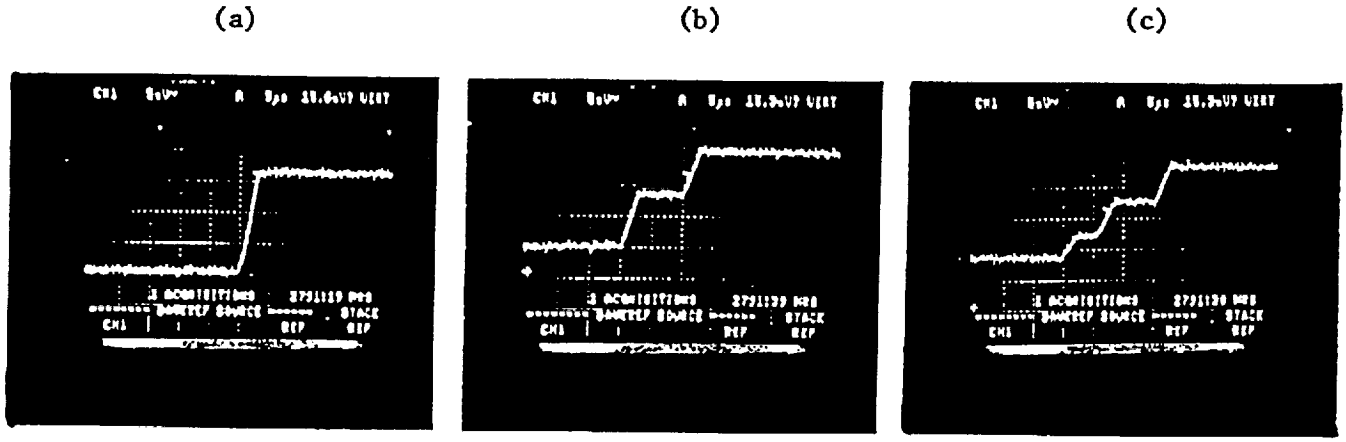

Fig. 5. Ionization pulses from ^{207}Bi 1.77 MeV γ-ray interactions in the 3.5 liter LXe chamber. (a) Single photoabsorption event. (b, c) Multiple Compton scattering events, followed by a photoabsorption.

As we know, Compton interaction is dominant in the few MeV region. The larger the depth of the liquid xenon, the greater the fraction of multiple-site events which contribute to the full energy peak. Monte Carlo simulation shows that for a γ-ray of 1 MeV in 6.0 cm of LXe, more than 50% of the interactions are from multiple Compton scatterings. All these interactions are separated in time by the propagation of the photon, but within the time scale of the detector they are simultaneous. The observation of the signal, however, takes place only after the drift time in the active volume, which depends on the location of the interaction point. Therefore, these multiple-site events are observed as multi-step features in the pulse shape. The height of the step gives the energy deposited at the point of interaction, and the time intervals between the steps give the relative distances of the interaction points, along the drift direction. The sum of all the step pulse-heights is proportional to the energy of the original γ-ray, if totally

absorbed. For example, based on the calibration of the charge sensitive preamplifier, the energy of all three events shown in Fig. 5 corresponds to 1.77 MeV γ-rays from the ^{207}Bi source. The information on the individual step pulse height and on the timing is very valuable. This timing, however, only gives information on the Z-coordinate of each site. By combining this with the additional information on the X-Y coordinates, event reconstruction based on Compton kinematics is possible as shown in reference. [2] This gives the capability of background identification and rejection. It also gives the capability to use a LXe-TPC as a Compton polarimeter of high sensitivity in the MeV energy range.

The overall energy resolution ΔE_t of the detector can be expressed as a combination of the following terms: the fluctuation in the number of electron-ion pairs produced ΔE_f, the electronic noise ΔE_e, the grid shielding inefficiency ΔE_s, the fluctuation in the collected charge due to recombination ΔE_r, and the variation of signal risetime ΔE_b. The full width at half maximum of the energy resolution can then be expressed as follows:

$$\Delta E_t^2 = \Delta E_f^2 + \Delta E_e^2 + \Delta E_s^2 + \Delta E_r^2 + \Delta E_b^2 \qquad (1)$$

The fluctuation of the electron-ion pairs is theoretically predicted as, $\Delta E_f^2 = (2.35)^2 FWE$ where W is the average energy required to create one electron-ion pair, F is the Fano factor, and E is the energy of the ionizing particle. The magnitude is about 0.2% FWHM at 1 MeV, a value which was experimentally never reached. The best observed value was 6% at 0.57 MeV.[6] An interpretation of the large discrepency is given elsewhere.[6]

The contribution from the electronic noise can be measured directly from the test pulse distribution. The typical noise contribution in our system is about 24 keV FWHM.

The grid shielding inefficiency contribution is estimated to be smaller than 1%.

The contribution of ballistic deficit, due to pulse rise time variation, is significant only in large volume detectors and can be minimized by appropriate signal processing.

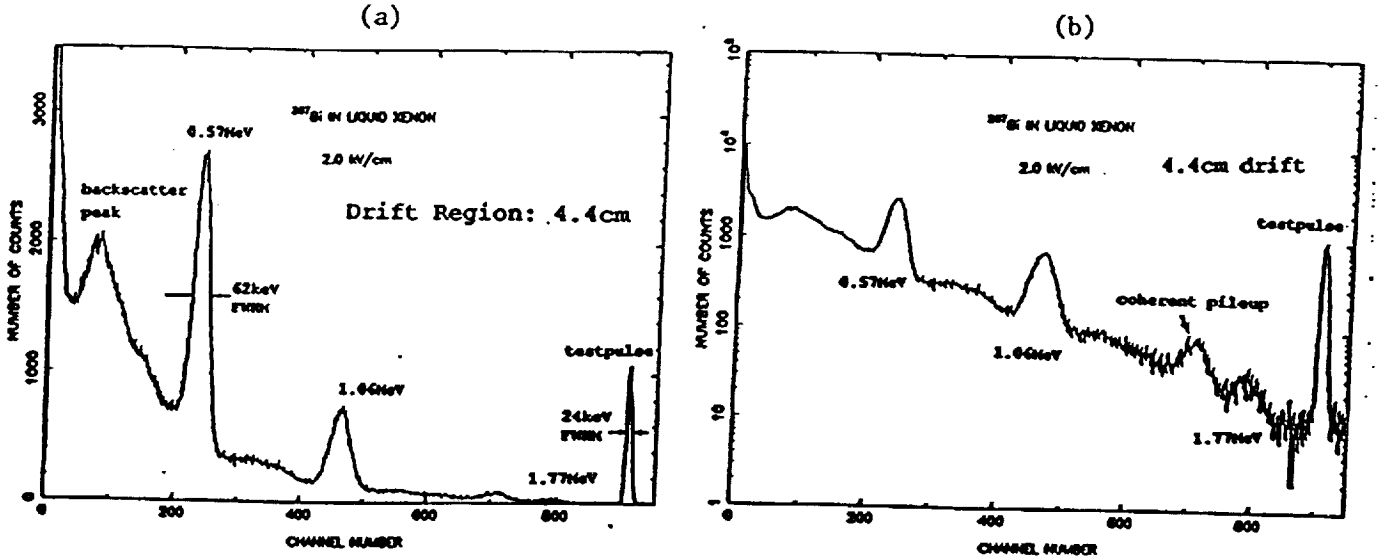

Fig. 6. (a) ^{207}Bi γ-ray spectrum recorded at 2 kV/cm with the 3.5 liter LXe chamber of 4.4 cm drift gap. (b) Same spectrum as that of Fig. 6a in semi-logarithmic scale.

In the case of a long drift LXe ionization chamber, the charge collection time can vary by more than 20 μs due to the multiple-site events. To completely collect all the charge, long shaping times are therefore required. This seriously reduces the speed of the detector, and also makes the measurement more sensitive to low frequency noise. Two solutions to the problem of ballistic deficit are: a) A gated integrator determining the total pulse height on-line. b) Waveform digitization and off-line reconstruction of the pulses.

The gated integrator solution is insensitive to rise time variations, as pointed out by Radeka.[7]

Fig. 6a shows the ^{207}Bi spectrum in the 3.5 liter chamber, obtained with a multi-channel analyzer after a 2 μs unipolar shaping of the signal, followed by a 2 μs gated integrator. Fig. 6b is the same spectrum in a semi-logarithmic scale. This spectrum was obtained with the drift gap reduced from 6.0 cm to 4.4 cm, in order to operate the chamber at high drift fields without voltage breakdown problems. The spectrum can be compared with that obtained earlier with much smaller chambers[6] where the maximun drift was few millimeters. The electronic noise subtracted energy resolution is compared in Fig. 7. Two important remarks can be made:

(a) The noise subtracted energy resolution of the large chamber is 10% at 0.57 MeV, comparable to that in the small chamber, at the same drift field. This means that fluctuation in the recombination process is the dominant factor of Eq. (1) which determines the measured resolution. It also means that the liquid purity was sufficient for long drift and that the signal processing with the gated integrator did not affect the resolution.

(b) Several peaks in the spectrum can only be observed in the large chamber due to its increased detection efficiency at high energies. Such features are the 1.77 MeV γ-rays, and the backscatter peak. A further feature is the peak at 1.63 MeV which is caused by 2 correlated events, i.e. a 0.57 MeV and a 1.06 MeV γ-ray emitted from the source simultaneously.

The gated integrator, however, reduces the detection efficiency, especially for high energy events, and also only conserves the total pulse height. The amplitude of each single step is lost. As previously mentioned, for a complete reconstruction of the event, the pulse height and position of each individual charge cloud are needed. These problems can be overcome by using a waveform digitizer on the anode without shaping of the original charge signal. Work on this method is under progress.

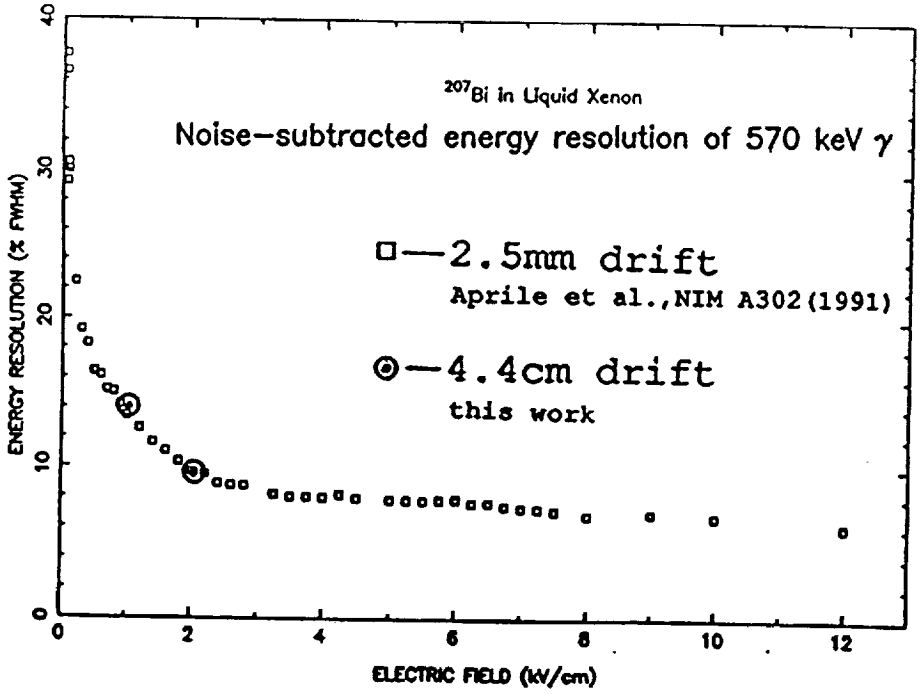

Fig. 7. Comparison of the noise-subtracted energy resolution of 570 keV γ-rays in LXe for 4.4 cm and 2.5 mm drift chambers.

3.2. Position Resolution Performance

The 3-D position resolution performance of a liquid xenon detector is largely determined by the read-out structure which is used to detect the signals induced by an ionizing event. In its simplest version, a system of two orthogonal

induction wire planes, separated from the drift region by a shielding grid, is used. The induced signals on the wires provide the X-Y information. The measured drift time, referred to a time zero, together with the known drift velocity, provides the Z-information. A single collection plate below the induction wires can be used for total charge collection. A preliminary design of the sensing electrodes geometry for 3-D imaging in a LXe-TPC as γ-ray telescope is shown in Fig. 8.

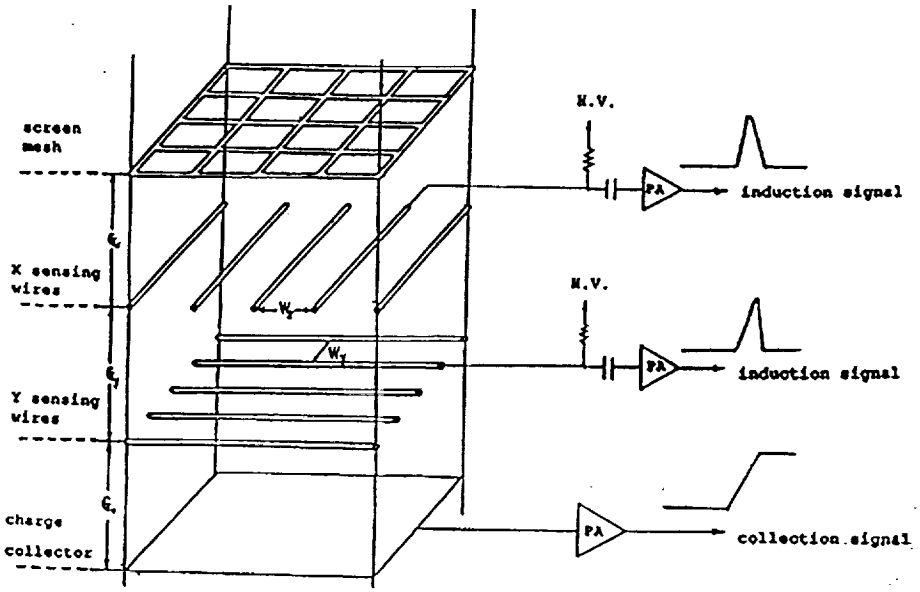

Sensitive Area:	40cm x 30cm
Wire Diameter:	50μm
Sreening Mesh:	500μm pitch, 50μm wire width
Spacing:	Wx=4mm, Wy=3mm, Gx=Gy=Go=2mm
Total Channels:	200 for X-Y sensing, 1 for calorimetry

Fig. 8. Schematic of the 3-D LXe-TPC electrode structure.

The time zero to the readout will be provided by the primary scintillation light signal[8] produced within a few nsec of the γ-ray interaction. This design is based on the original one by Gatti et al.[9] These authors calculated the induced waveforms for this type of readout structure and showed (Fig. 9) that the amplitude of the signal produced by a point-like ionization depends strongly on the initial lateral position of the cloud between the sense wires. It was reported[10] that this effect is undesirable for tracking charged particles. For the gamma-ray application of a LXe-TPC, however, tracking capability is not needed since the density of the liquid is such that the small energy depositions produced by gamma-ray interactions result in localized or point-like charge blobs, in a detector with a practical wire spacing of the order of millimeters.

Actually this dependence of the induction signals on the position of the charge blobs with respect to the wires, can be an advantage for the spatial resolution. The location of a point charge can in fact be determined with a smaller error by weighing the signals from adjacent wires to obtain the center of gravity of the charge cloud. Without determining the center of gravity, the position of the cloud is determined from the location of the sense wire, and the error in localization of the cloud is $s/\sqrt{12}$, where s is the wire spacing. Using the signals from two adjacent wires to estimate the position reduces this error. Now the error is dominated by the accuracy of the amplitude measurement, i.e. the signal-to-noise ratio. Obviously, a smaller wire spacing still increases the position resolution, but cost and complexity considerations will limit the overall number of wires.

These considerations were tested with the 2-D 3.5 liter TPC prototype shown in Fig. 2, with the electric field lines as shown in Fig. 3. The first measurements were dedicated to the observation of the induction signal on the sense wires. Fig. 10 shows the induction signal produced by a ^{207}Bi γ-ray event, and the corresponding collection

signal recorded simultaneously.

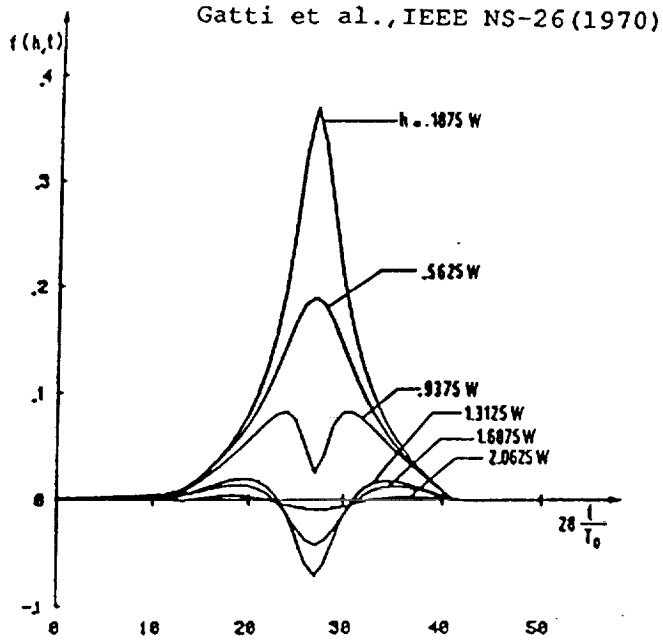

Fig. 9. The calculated induction waveform for a point-like charge at different lateral positions h from the sense wires spaced by W.

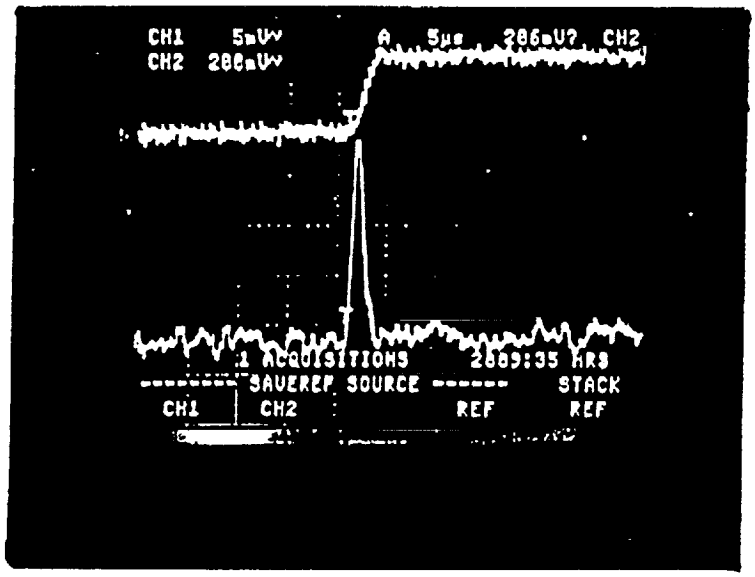

Fig. 10. Charge signal produced by a γ-ray event in the 2-D LXe-TPC. Upper trace: collection signal on anode (gain=1); Lower trace: induction signal on sense wire (gain=400).

The signal from the sense wire was used as the trigger. The induction signal was amplified by a gain of 400, while the gain of the collection signal was unity. For this event, the induced charge is $\sim$ 30% of the total collected charge, implying that the single γ-interaction point was close to the sense wire, based on Fig. 9. The induction signal has the same time duration as that of the collection signal, as expected. The induction signal has the expected triangular shape (see Fig. 9). It is not symmetric due to the shorter distance between the screening grid and the sense wires, than that between the sense wires and the collector. The signal-to-noise ratio is 12:1. This is sufficient

to significantly improve the position resolution inferred from the time information.

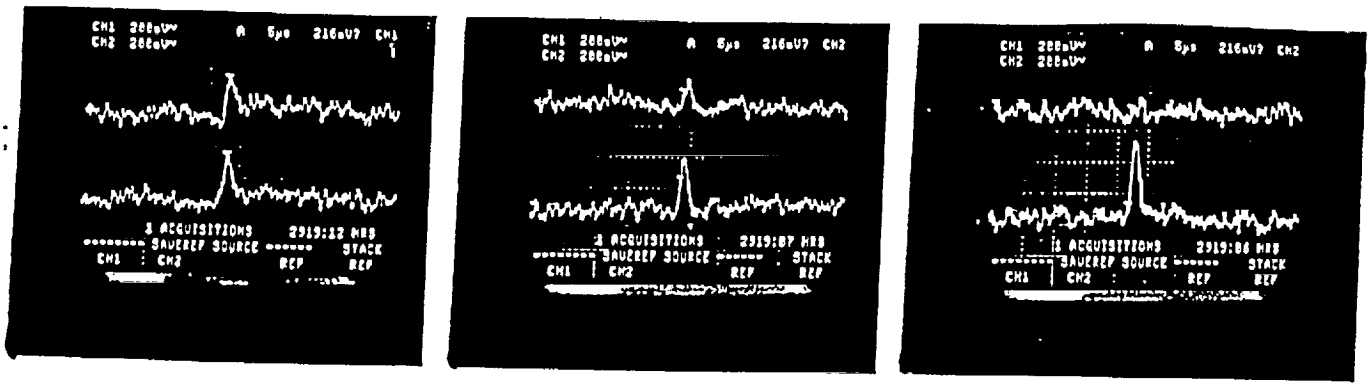

Fig. 11. Induced signals on neighboring wires observed in the 2-D LXe-TPC for different γ-ray events.

We also investigated the induction signals induced simultaneously on neighboring wires. As shown in Fig. 11, the relative amplitude of the signals changes on an event-by-event basis, indicating the different lateral positions of the charges produced by γ-ray interactions. This clearly demonstrates the potential to achieve a better spatial resolution on the X-Y coordinates than that determined by the wire spacing.

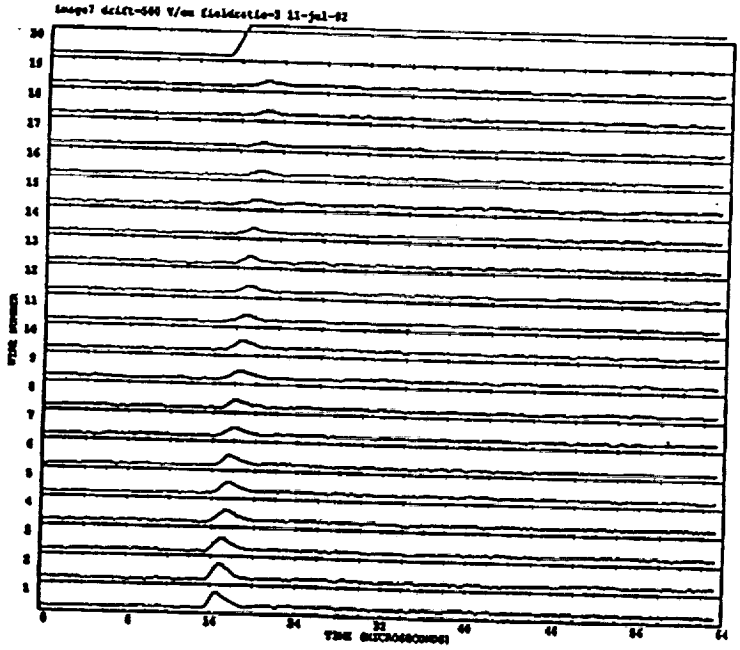

Fig. 12. Cosmic muon track observed with the 2-D LXe-TPC in induction mode.

Previously, the tracking capability of a 2D LXe-TPC was reported by using a a segmented anode, read-out in collection mode.[11] With the present structure, charged particle tracks have been observed in the induction mode. Fig. 12 shows the signals induced on the sense wires by a cosmic muon passing through the chamber and depositing, successively, energy on all wires.

The signal from the anode, shown on channel 20 of Fig. 12, was used as the trigger. The timing of the signals

can be converted into drift length, and provides the coordinate of an ionizing event along the drift direction. Due to the triangular pulse shape, the determination of an accurate timing is easier than for the signal shape observed earlier in collection mode. This fact, together with the better signal to noise ratio, will improve the spatial resolution in this direction from the previously measured 180 μm[11]. The analysis of these data is still in progress. Intrinsically, the localization of the charge cloud is ultimately limited by electron diffusion along the drift path which causes a spread of the cloud. In the drift direction, a spatial resolution close to the diffusion limit can be expected. The final value depends on the accuracy on the timing of the pulses, limited in practice by the signal-to-noise ratio. The lateral diffusion, orthogonal to the drift direction, is given by $\sqrt{Dt_d}$, where D=65 cm^2s^{-1} is the diffusion coefficient[12], t_d is the drift time. For drift distances of maximum 10 cm, as in the proposed LXe-TPC telescope, the resulting value is negligible when compared with the spacing of the sense wires.

4. CONCLUSION

A γ-ray telescope for the energy range from 0.3 MeV to 10 MeV was proposed to measure the γ-ray flux from galactic sources in balloon borne experiments. The telescope is based on a LXe-TPC as 3-D position sensitive detector and spectrometer, coupled to a coded aperture mask. The active area is 1200 cm^2 and the maximum drift length 10 cm. The size of this TPC is considerably larger than liquid xenon detectors tested so far. To achieve the desired performance of the telescope, it is mandatory to measure the energy and position of all γ-ray interaction points produced by multiple Compton scatterings.

To evaluate the feasibility, a 3.5 liter prototype was constructed and repeatedly operated. The required purity level for the xenon gas was achieved with a simple purification system, of the type used for previous measurements with liquid xenon small volume detectors.

The prototype was tested in a gridded chamber configuration with 4.4 cm drift gap, for charge collection and energy resolution studies. With this large sensitive volume detector, the enhanced detection efficiency of liquid xenon for γ-rays is clearly visible. Despite the much longer drift distance, the noise-subtracted energy resolution measured with this detector is comparable, at the same electric field of 1 and 2 kV/cm, to that previously measured with smaller size chambers.

The feasibility of a non-destructive electron imaging of ionization events with a liquid xenon TPC was established. For this purpose, the readout structure consisted of an induction plane of sense wires to provide the position information and a collector plate for total charge collection. The induced signals produced by MeV γ-rays and cosmic ray muon tracks on sense wires have been observed, for the first time, in liquid xenon. A large signal-to-noise ratio was achieved and the pulse shape and timing of the induction signals were consistent with expectation. For the final detector, a position resolution better than $s/\sqrt{12}$ can be expected, where s is the wire spacing. Along the drift direction, the resolution will be better than 180 μm measured earlier, since a more accurate timing is possible on the induced waveforms, and due to the improved signal to noise ratio.

5. ACKNOWLEDGEMENTS

This work was supported by NASA grant NAGW-2013 and partially by NSF grant PHY-91-09937. We also would like to thank many colleaugues, and in particular D. Schinzel, V. Radeka, S. Rescia and F. Pietropaolo for support and valuable discussions.

6. REFERENCES

1. E. Aprile et al., "A High Resolution Liquid Xenon Imaging Telescope for 0.3 – 10 MeV Gamma-Ray Astrophysics: Construction and Initial Balloon Flights," NASA proposal, CAL-2015 (1992).

2. E. Aprile et al., "A Monte Carlo Analysis of the Liquid Xenon TPC as Gamma-Ray Telescope," to be published in *Nucl. Instr. and Meth. A* (Aug.1992).

3. E. Aprile, R. Mukherjee, and M. Suzuki, "EUV, X-Ray and Gamma-Ray Instrumentation for Astronomy and Atomic Physics," *SPIE Conference Proceedings*, ed.C.J. Hailey and O.H.W. Siegmund, **1159**, (1989) 295.
4. E. Aprile, R. Mukherjee and M. Suzuki, *Nucl. Instr. and Meth.*, **A300**, (1991) 343.
5. O. Bunemann, T.E. Cranshaw and I.A. Harvey, *Can. J. of Res.*, **27** (1947) 191.
6. E. Aprile, R. Mukherjee and M. Suzuki, *Nucl. Instr. and Meth.*, **A302** (1991) 177.
7. V. Radeka, *Nucl. Instr. and Meth.*, **99** (1972) 525.
8. E. Aprile, R. Mukherjee and M. Suzuki, *IEEE Trans. Nucl. Sci.*, **NS-37**, (1990) 553.
9. E. Gatti et al., *IEEE Trans. Nucl. Sci.*, **NS-26**, (1970) 2910.
10. E. Bonetti et al., *Nucl. Instr. and Meth.*, **A286** (1990) 135.
11. E. Aprile et al., *Nucl. Instr. and Meth.*, **A316**, (1992) 29.
12. E. Shibamura, et al., *Phys. Rev.*, **A20**, (1979) 2547.